Insights into Congo Red Adsorption on Agro-Industrial Materials - Spectral, Equilibrium, Kinetic, Thermodynamic, Dynamic and Desorption Studies. A Review

Zvezdelina L. Yaneva, Nedyalka V. Georgieva

Abstract – *The present review highlights and provides an overview of the equilibrium, kinetic, dynamic and thermodynamic studies of Congo red (CR), a diazo carcinogenic dye, adsorption on various agricultural by-products, wastes and agro-industrial residues. The effect of some significant parameters such as pH, temperature, ionic strength, initial sorbate concentration, contact time, etc. on the adsorption behaviour of the studied systems was outlined. Insights into the mechanism of the sorption processes applied were presented and analyzed on the bases of: (i) the lignocellulosic sorbents physicochemical properties (specific surface area, pore size, surface functional groups), spectral (FTIR), morphological characteristics and adsorption capacity; (ii) the structural complexities and UV/VIS spectra of the dye macromolecule, and (iii) the subsequent alterations of sorbate/sorbent electrostatic, physical and chemical interactions throughout the entire sorption process. Besides, comprehensive analyses of the applicability of a number of equilibrium, kinetic, mass-transfer and dynamic mathematical models were presented. The available in the literature studies subjected to CR desorption were also summarized, as they present strategies for the future regeneration, reuse and utilization of the exhausted adsorbents and assist the elucidation of the process mechanism(s).* **Copyright © 2012 Praise Worthy Prize S.r.l. - All rights reserved.**

Keywords: Adsorption, Congo Red, Lignocellulosic Agro-Industrial Materials, Mechanism

I. Introduction

Out of all contaminants contained in industrial sewage, dyes are the most undesired ones, as the direct discharge of dye effluents can cause serious problems to the environment due to contribution of high organic loading, toxicity and aesthetic pollution related to colour [1].

Azo dyes are the largest class of dyes with the greatest variety of colours - approximately 10–15 % of the dyes are released into the environment during dyeing of different substrates, such as synthetic and natural textile fibres, plastics, leather, paper, mineral oils, waxes, and even foodstuffs and cosmetics [2]. They exhibit great structural variety, thus they are not uniformly susceptible to microbial attack. Azo dyes are not typically degraded under aerobic conditions; however, under anaerobic conditions, the azo linkage can be reduced to form aromatic amines which are colourless but can be toxic and carcinogenic [3]. Azo dyes and their pigments are also typically amenable to structural modification and representative azo dyes can be made to bind most synthetic and natural textile fibers. Several amino-substituted azo dyes including 4-phenylazoaniline and N-methyl- and N,N-dimethyl-4-phenylazo anilines are mutagenic and carcinogenic.

In mammals, azo dyes are reduced to aryl amines by cytochrome p450 and a flavin-dependent cytosolic reductase [4].

Azo dyes consist of a diazotized amine coupled to an amine or a phenol and contain one or more azo linkages.

The criterion of harmfulness of benzidine based dyes is the possibility of splitting into carcinogenic amines [5]. It was determined that approximately 130 of 3,200 azo dyes in use have produced carcinogenic aromatic amines as a result of reductive degradation [6].

These amines have been defined as the so-called Maximal Arbentsplatz Konzentration (MAK) III A1 amines (e.g. benzidine, β-naphthylamine) and MAK III A2 amines (e.g. *o*-toludine) [7], as well as International Agency for Research and Cancer (IARC) and Ecological and Toxicological Association of the Dyestuffs Manufacturing Group (ETAD) 1 (4-amiobiphenyl,2-Naphthylamine). Several European countries, mainly, including Germany definitely forbid the presence of MAK amines in textile products.

Currently, all the European Union legal and customs regulations which are being prepared follow this trend and prohibited the manufacture and sale of benzidine based azo dyes from September 2003 [8],[9].

In Turkey the Turkish government banned the utilization of 130 azo dyes from 1 March 1995 due to

relevant aromatic amines and prohibited the use of these dyes in the textile market.

However, they are still used in textile dyeing processes due to their efficiency of dying and cost [2]. In a world of rapid assimilation of natural resources, any attempt of the utilization of agricultural wastes and by-products augments the raw material stock and also provides additional employments and income to marginal farmers and landless agricultural laborers, especially in developing countries [10]. Agricultural by-products, wastes and agro-industrial residues are lignocellulosic materials that consist of three main structural components: lignin, cellulose and hemicelluloses [11].

Agricultural wastes are renewable, available in large amounts and less expensive as compared to other materials used as adsorbents. Some of them have been used without or with a minimum of processing (washing, drying, grinding) and thus reduce production costs by using a cheap raw material and eliminating energy costs associated with thermal treatment [12]. Others were physically or chemically modified to achieve better adsorption characteristics and to elucidate the adsorption process.

The physical treatments include heating/boiling, freezing/thawing, lyophilization. The chemical modification techniques include washing with detergents, cross-linking with organic solvents, alkali or acid treatment, chemical reaction with various organic/inorganic compounds, and microwave-assissted modification [10]-[25]. The pretreatments modify the surface characteristics/groups either by removing or masking the groups or by exposing more active binding sites [26]. Thus, degraded cells offer a larger available surface area and intracellular component. The destruction of the cell membranes increases the availability of more surface binding sites and alters changes in the functional groups present on the cell wall [27].

The present review paper highlights the physicochemical, spectral, equilibrium, kinetic, dynamic and thermodynamic aspects of Congo red adsorption on various agro-industrial materials, depicting the effect of a number of factors on the mechanism of the process and the probable sorbate/sorbent interactions.
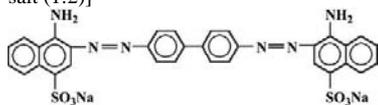
II. Congo Red (CR) - Chemistry and Environmental Fate

II.1. Physicochemical Characteristics and Toxicity

Congo red (CR) is a benzidine-based, direct, anionic diazo dye prepared by coupling tetrazotised benzidine with two molecules of napthionic acid. Its molecular structure and physicochemical characteristics are presented in Table I. Congo red is the first synthetic azo dye produced that is capable of dying cotton directly. Congo red containing effluents are generated from a number of industrial activities: textiles, printing and dyeing, paper, rubber, plastics industries [30],[31],

production of display devices, optical films, alignment layers, fiber-optic sensors, optical waiveguides, highlighters, etc. [28]. Besides, CR has been widely used for staining (amyloid-β protein, bacteria, carious tissue, collagen, fungi, fungal cell wass mutants; liposome; polyglutamine protein oligomers, prion, skin, α-synuclein, etc.) and biological applications (detecting bacteria; protein folding disorders; treating dermathological disorders; neurodegenerative diseases, Alzheimer's desease, etc.) [28].

TABLE I
PHYSICOCHEMICAL CHARACTERISTICS OF CONGO RED [28],[29]

CAS No.	573-58-0
CA Index name	1-Naphthalenesulfonic acid, 3,3'-[(1,1'-biphenyl)-4,4'-diylbis(2,1-diazenediyl)]bis[4-amino-,sodium salt (1:2)]
Chemical structure	
Molecular formula	$C_{32}H_{22}N_6Na_2O_6S_2$
Molecular weight	696.66 g mol^{-1}
Molecular surface area	557.6 Å^2
Physical form	brounish-red powder
Solubility	soluble in water, ethnol; very slightly soluble in acetone; practically insoluble in ether, xylene
Density	0.995 g cm^{-3} at 25°C
Other names	3,3'-[[1,1'-biphenyl]-4,4'-diylbis (azo)]bis[4-amino-1-naphthalenesulfonic acid]disodium salt; 1-naphthalenesulfonic acid,3,3'-[[1,1'-biphenyl]-4,4'-diylbis-(azo)]bis[4-amino, disodium salt]; C.I. Direct Red 28, disodium salt; Atlantic Congo Red; Atul Congo Red; Azocard Red Congo; Benzo Congo Red; Brasilamina Congo 4B; Cerven Congo; Cerven Prima 28; C.I. 22120; C.I. Direct Red 28; Congo Red 4B; Congo Red 4BX; Congo Red CR; Congo Red H; Congo Red K; Congo Red L; Congo Red M; Congo Red N; Congo Red R; Congo Red RS; Congo Red TS; Congo Red W; Congo Red WS; Congo Red sodium salt; Congo Red; Cotton Red 4BC; Cotton Red 5B; Cotton Red L; Congorot; Diacotton Congo Red; Direct Congo Red; Erie Congo 4B; Haemomedical; Haemonorm; Hemorrhagyl; Hispamin Congo 4B; Kongorot
Dye Class	Azo
Melting point	> 360°C
pH range	3.0-5.0
Colour	Blue (pH 3.0) to red (pH 5.0)
pKa	4.1; 3.0
Absorption wavelenght (λ_{max})	497 nm; 488 nm

Exposure to the dye has been known to cause allergic reactions. The substance is considered as toxic exhibiting acute, algal, bacterial, protozoan, cutaneous, environmental, microbial, yeast toxicity; cytotoxicity; genotoxicity; hematotoxicity; neurotoxicity, as well as carcinogenicity and mutagenicity [28],[32],[33]. The capability of CR to form carcinogenic amines such as benzidine through cleavage of one or more azo groups is the reason why it falls under the category of banned azo dyes [34]. The recalcitrance of CR has been attributed to

the presence of aminobiphenyl group and azo bonds, two features generally considered as xenobiotic [2],[35].

Thus, the treatment of CR contaminated wastewater can be complicated due to its complex aromatic structure, providing the dye physicochemical, thermal and optical stability, and resistance to biodegradation and photodegradation [30],[31],[36]. Consequently, due to the harmful effects of this organic compound, the wastewaters containing CR must be treated before being discharged to receiving water bodies.

The secondary biological processes are commonly used for domestic and industrial wastewater treatment, but their efficiency is not satisfactory at high pollutant concentrations [37]. Therefore, the efforts have been directed to the development of new treatment technologies such as: ozonation [38],[39], enzyme-based decolourization [40], photocatalytic degradation [41]-[44], sonochemical degradation [45,46], microwave-assissted degradation [25], degradation by sunlight/Fe^{2+}/$S_2O_8^{2-}$ method [47], biodegradation [48], electrochemical oxidation [39],[49],[50], catalytic wet peroxidation [51], coagulation with naturally prepared coagulants: surjana seed powder (SSP), maize seed powder (MSP) and chitosan [52], etc.

All these processes have their own limitations and advantages. The removal of dyes and organics in an economic way, however, remains an important problem although a number of systems have been developed with adsorption technique. Adsorption is a very effective separation technique and now it is considered to be superior to other techniques for water treatment in terms of initial cost, simplicity of design, ease of operation and insensitiveness to toxic substances [53]-[55]. In this process the dye species are transferred from the water effluent to a solid phase that leads to decreasing the effluent volume [56],[57]. In order to assess the fate of CR in wastewater and to control its mobility and reactivity during remediation processes, the sorption behaviour of this toxic contaminant must be understood and revealed. Although carbon adsorbents are very versatile due to their high surface area, well-developed pore structure and surface properties [58], there are economic objectives, namely high cost and need for regeneration after saturation, that restrict their applicability for wastewater treatment [59]. Literature reports many works concerning the optimization of CR adsorption by developing new low-cost adsorbent products (clay minerals, industrial by-products/waste materials, biomass, different soil types, etc.) and elucidating the mechanism of the process. Suitable alternatives are summarized in Table II.

II.2. Spectrophotometric Analyses and Protonation Pathways of CR

Congo red contains an azo (-N=N-) chromophore and an acidic auxochrome (-SO$_3$H) associated with the benzene structure. CR is also called acidic diazo dye.

The azo structure is more important because of its high ability to impart colour to the compound [18]. CR in aqueous solution exhibited a main band at λ 488-500 nm (pH ~ 8), assigned to the absorption band of anionic monomer, and associated with two absorption bands in the UV-region at λ 235 and 347 nm, attributed to the benzoic and naphthalene rings, respectively. The CR monomers have nearly constant absorption bands and absorbance intensities over the pH range 6 - 10, which means that the aggregation did not occur, while they are most sensitive to the pH solution under acidic medium (pH < 6).

The main band of CR monomer at λ 488-500 nm (in aqueous solution) gradually shifts to the longer wavelengths, almost reaching 595.5 and 537.5 nm at pH 2 and 4, respectively [80],[81]. The intensity decreases and red shift of CR monomer bands are attributed to the partially self-association of CR monomers as anionic dimers in face-to-face arrangement to minimize their hydrophobic interaction with water. For that reason, the adsorption and photocatalytic degradation investigations of Nadjia et al. [80] were conducted only within the neutral and alkali pH range. At pH > pH$_{PZC}$ (point of zero charge) of the adsorbent, the solid surface is negatively charged and repels R-SO$_3^-$ ions. Furthermore, dye molecules in acidic or highly acidic pH ranges tend to aggregate and form tautomerism state. While it is known that azo dyes undergo a protonation process in acid solutions, the protonation sites have been disputed. CR has four N atoms that can be potential protonation sites, and thus there are different possible types of protonated dye molecules [82]. Protonation of CR could be occurring at amino (Fig. 1, structure II) or azo nitrogens (Fig. 1, structure III).
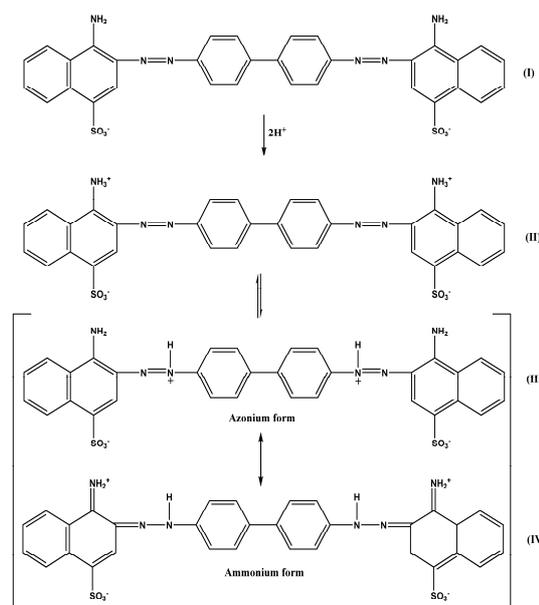

Fig. 1. Mechanism of Congo Red protonation in aqueous media. Adapted from [81],[82]

TABLE II
ADSORPTION CAPACITIES AND EXPERIMENTAL CONDITIONS OF VARIOUS NATURAL AND SYNTHETIC ALTERNATIVE ADSORBENTS
FOR CONGO RED REMOVAL

Adsorbent	BET surface area, S_{BET}, m^2 g^{-1}	Adsorption capacity, q, mg g^{-1}	Temperature, T, ^oC	pH	Concentration, C_o, mg L^{-1}	Ref.
kaolin	20.28	5.60	25-60	3-11	150-1000	[25]
Australian kaolins:						
Q38	20.28±0.02	5.62	25-60		50-250	[55]
K15GR	16.21±0.04	6.92				
Ceram	26.69±0.02	8.97				
Na-bentonite	25.70	19.90	25-60	3-11	150-1000	[25]
CaCl$_2$ bentonite	-	227.27	25-60	5-10	100-150	[56]
bentonite	28.00	158.7	25±2	3-11	75-300	[57]
raw bentonite	25.7±0.08	20.8	25-60	3-11	100-1000	[58]
thermally activated bentonite (TA)	75.5±0.10	52.6	25-60	3-11	100-1000	[58]
acid activated bentonite (AA)	34.6±0.06	61.5	25-60	3-11	100-1000	[58]
acid-thermally activated bentonite (ATA)	84.6±0.12	74.5	25-60	3-11	100-1000	[58]
zeolite	8.31	4.30	25-60	3-11	150-1000	[25]
clay mixtures:						
Mixture 1 (65% Ca(OH)$_2$+15% Na-bentonite+15% kaolin+5% zeolite)	20.7	575.49			40-600	
Mixture 2 (70% Ca(OH)$_2$+15% Na-bentonite+10% kaolin+5% zeolite)	25.1	586.51		3-11		[59]
Mixture 3 (70% Ca(OH)$_2$+10% Na-bentonite+10% kaolin+10% zeolite)	19.6	583.43				
native and modified mycelial pellets of *Trametes versicolor*	-	10-51.81 (autoclaved) 10.00-42.35 (live) 6.85-26.16 (acid pretreated) 6.11-22.42 (alkali pretreated)	-	-	10-50	[16]
Penicillium YW 01 biomass	-	411.53	20-40	1-10	50-800	[60]
commercial activated carbon (CAC)	492	48.70-183.10	30 - 50	2-12	50-545	[26]
coal-based mesoporous activated carbon	370-679	52-189	-	7.8-8.3	50	[61]
marine algae (*Valoria bryopsis)* activated carbon	-	3.40-10.5		1-7	10-30	[62]
magnetic cellulose (Fe$_3$O$_4$) activated carbon	11.8669	66.09	25-55	4-9.5	5-70	[63]
Pd nanoparticles loaded activated carbon (Pd NPs-AC)	-	76.9	10-60	6	15-25	[64]
Ag nanoparticles loaded activated carbon (Ag NPs-AC)	-	66.7	10-60	4-7	15-25	[64]
ZnO nano rods loaded activated carbon (ZnO NRs-AC)	-	142.9	10-60	7	15-25	[64]
Ni(OH)$_2$ nanosheets	127	82.9	25	7	15-50	[65]
NiO nanosheets	201	151.7	25	7	15-50	[65]
NiO nanoparticles	2.5	39.7	25	7	15-50	[65]
biogas waste slurry	-	9.50	-	2.3-9.4	-	[66]
waste red mud	-	4.05	-	2	-	[66]
acid activated red mud	20.7	7.08	-	7	10-90	[12]
electrocoagulated metals hydroxide sludge (EMHS)	-	271-513	-	3-10	100-300	[68]
cambic chernozem soil (Romanian)	-	2.24	-	-	-	[31]
sandy loam, loam and clay Greek soils	-	0.500-0.625	-	4-12	25-125	[69]
open burnt clay	-	22.83	26±2	2-12	-	[15]
chitosan	-	78.90	-	4-9	200-1000	[16]
N,O-carboxymethyl-chitosan	-	579.00	30-50	4-9	200-1000	[16]
chitosan/montmorillonite (CTS:MMT = 5:1) nanocomposites	22.3	54.52	30-50	4-9	200-400	[70]
waste Fe(III)/Cr(III) hydroxide	-	44.00	-	-	-	[71]
chitosan hydrobeads	-	93.00	20-50	3-12	1-500	[24]
surfactant-modified montmorillonite	-	31.10-127.00	30-50	4-9	800-1000	[18]
HTMAB-modified attapulgite	-	189.39	30-50	4-9	200-600	[19]
eggshells	-	69.45	40	6.0	50.00	[72]
nanocrystalline MFe$_2$O$_4$ (M = Mn, Fe, Co, Ni) spinel ferrites	-	30.7-170.2	18	7.0	50-150	[73]
anilinepropylsilica xerogel	150	22.62	25	2-12	4-120	[74]

Structures III and IV represent two distinct resonance structures. In fact, it has been reported that in protonated azo compounds having amino groups there is an equilibrium mixture of two tautomers, i.e. the ammonium and azonium ions (Fig. 1). Probably protonation in amino sites bonded to naphtyl rings, changes the

electronic distribution of the aromatic ring, thus leading to quinoid-like form (Fig. 1, structure IV) [81],[82].

III. Physicochemical, Spectral and Morphological Characteristics of the Adsorbents

To understand the adsorption mechanism, it is necessary to determine the concentrations of the surface active groups, the point of zero charge (pH_{PZC}) of the adsorbent and to analyze changes in the sorbent spectra before and after adsorption, as well as in the surface morphology of the fresh and dye-loaded adsorbents. Adsorption of cations is favoured at $pH > pH_{PZC}$, while the adsorption of anions is favoured at $pH < pH_{PZC}$ [19].

Ahmad and Kumar [83] studied the adsorption of CR onto bael shell carbon (BSC) and investigated the proper adsorption mechanism. Bael (*Aegle marmelos*) is an indigenous fruit of India. The Scanning electron microscopy (SEM) images showed irregular and porous texture surface morphology. The pores were prominent on the surface of the fresh BSC but after adsorption the pores were filled by the dye molecules, showing the adherence to the surface of the adsorbent. The concentrations of total acidic and basic sites on BSC determined by the Boehm titration method were 0.64 mequiv g^{-1} (carboxylic and lactonic site – 0.52 mequiv g^{-1} and carboxylic site – 0.12 mequiv g^{-1}) and 0.3 mequiv g^{-1}, respectively [83]. According to Wang and Wang [19] adsorption of cations was favoured at $pH > pH_{PZC}$, while the adsorption of anions was favoured at $pH < pH_{PZC}$. The pH_{PZC} of BSC was 6.28 [83].

Mishra et al. [89] explored the potential of another new agricultural waste material that is available in plenty in Orissa, India i.e. Mahua oil cake (MOC) as an adsorbent for CR removal. The authors established that MOC is composed of cellulose (60.42 %), lignin (20.21 %) and hemicelluloses (16.21 %). The BET surface area was 2.24 m^2 g^{-1}. The SEM micrographs of MOC samples before and after CR dye adsorption displayed considerable number of porous sites that indicated a good possibility for the dye to be trapped and adsorbed. The pH_{PZC} of MOC was 6.2 [84].

Rice husks contain abundant floristic fiber, protein and some functional groups such as carboxyl, hydroxyl, amidogen, etc., which make the adsorption processes possible [85]. Furthermore, the yield of rice husk obtained from agriculture as a byproduct is vast. Hence rice husk is low cost and can be easily obtained [32]. In the study of Sarkar et al. [86], the surface morphology of Rice husk ash (RHA) obtained by SEM clearly indicated the presence of irregular and highly porous structure of the sample studied. Reddy et al. [87] investigated the feasibility of using unmodified Indian Jujuba Seeds (IJS) (*Zizyphus maruritiana*) as a low cost and eco-friendly adsorbent for CR removal from aqueous solution. The pH_{PZC} of IJS was 7. The SEM analyses displayed that IJS contained considerable number of heterogeneous pore layers. The FTIR spectrum of IJS and CR loaded IJS is presented in Table III(A). The changes observed in the spectrum indicated the possible involvement of those functional groups on the surface of the IJS (*Z. maruritiana*) during the adsorption process [87]. Panda et al. [88] proved that Jute stick powder (JSP) could be successfully applied as a promising adsorbent for CR and rhodamine B removal from aqueous solutions. The specific surface area of JSP determined by a BET surface area analyzer was 32.6 m^2 g^{-1}. The SEM analysis of the pristine JSP outlined a smooth and layered structure over a large area corresponding to dye–surface interactions. Significant changes in the surface morphology were noted, which became uneven and irregular after adsorption of CR and rhodamine B. The relatively thick layer of rhodamine B on JSP surface supported the greater adsorption capacity (87.7 mg g^{-1}) of the biomass when compared to that of CR adsorption (35.7 mg g^{-1}). The FTIR spectrum for pristine JSP biomass was recorded and presented in Table III(A) [88].

Alternanthera bettzichiana (Regel) Nicols plant powder (ABPP) was investigated as a low cost and eco-friendly adsorbent for CR removal from aqueous solution [89]. Examination of SEM micrographs of the ABPP showed rough areas of the surface and identifiable micropores. The elemental analysis of the sorbent by Energy-dispersive X-ray spectroscopy (EDAX) indicated 53.62 % C, 29.30 % O and 17.04 % N content before adsorption and 61.05 % C, 20.34 % O and 18.61 % N - after adsorption. According to the FTIR spectral analysis of fresh and dye-loaded ABPP (Table III(B)), it was established that the main functional groups involved in adsorption process were carbonyl, carboxyl, alcoholic and amino groups [89].

The leaves of *Azadirachta indica* (Neem tree) in the form of a powder were investigated as a biosorbent for CR removal from its model aqueous solutions [90]. The sorbent was made from mature Neem leaves and was investigated in a batch reactor under variable system parameters. An amount of 0.6 g L^{-1} Neem leaf powder (NLP) could remove 52.0–99.0 % of the dye from an aqueous solution with initial concentration 2.87×10^{-2} mmol L^{-1} with agitation time increasing from 60 to 300 min [90].

Cashew nut shells (CNS) - a novel, low cost adsorbent prepared from agricultural waste was utilized for CR the removal from aqueous medium by Kumar et al. [91]. CNS were collected from Pudukkottai District, Tamilnadu, India, and used as an adsorbent without any preliminary physical or chemical modification. The BET surface area, pore volume, average pore diameter and bulk density of the CNS were: 395 m^2 g^{-1}, 0.4732 cm^3 g^{-1}, 5.89 nm and 0.415 g cm^{-3}, respectively. The analyses of CNS FTIR spectra before (Table III(B)) and after CR adsorption revealed that after CR sorption the peaks of – NH and $-NH_2$ disappeared; –NH rocking peak shifted to a higher wave number, indicating the significant role of amine groups in the adsorption process; the stretching

vibration of the second –OH group shifted to a lower wave number; vibration for the first –OH group did not change much. Consequently, the -NH$_2$ and the second –OH groups were probably included in the adsorption of CR [91].

The study of Hu et al. [92] investigated the removal of CR by cattail root from aqueous solution. Cattail is an aquatic plant and has been widely used in artificially constructed wetlands for the removal and mineralization of phenol [93], the treatment of high-strength wastewater [94], and the removal of phosphorous and heavy metals [95]. However, the cattail biomass and its root produced in the phytoremediation probably would become a potential pollution source like water hyacinth if they are not properly managed. Due to its porous structure and large surface area, cattail root was utilized as an adsorbent to treat CR contaminated wastewaters [92].

Annadurai et al. [96] tested the possibility of using cellulose-based wastes: banana and orange peels, for adsorptive removal of various dyes (methyl orange, MO; methylene blue, MB; Rhodamine B, RB; methyl violet, MV; amido black 10B, AB) including CR from aqueous medium. The BET surface areas of both types of peels were in the range 20.6–23.5 m^2 g^{-1}. The SEM images of fresh banana and orange peels showed that the pores within the peel particles were highly heterogeneous. After CR adsorption, however, the peels appeared to have a rough surface with crater-like pores due to the partial coverage by the dye macromolecules [96].

Zhang et al. [97] presented a comprehensive study on CR adsorption by ball-milled sugarcane bagasse - a type of lignocellulosic material that is abundant and readily transportable waste product from the sugar manufacturing industry. The depithed bagasse consisted of 42.9 wt % cellulose, 27.1 wt % hemicelluloses, 27.0 wt % lignin and 0.4 wt % ash. The pH$_{PZC}$ of bagasse was 5.0. The surface area of the cutter grinded samples varied from 0.58 m^2 g^{-1} to 0.66 m^2 g^{-1}, while that of the ball-milled samples was increased to 1.31–1.82 m^2 g^{-1}. The values of the crystallinity index estimated by X-ray powder diffraction (XRD) analysis ascertained that ball milling increased the surface area, and significantly reduced the crystallinity of the cellulose component from 0.6 for cutter grinded samples to 0.15 for ball-milled samples. Based on the observed differences between the FTIR spectra of bagasse before and after CR adsorption (Table III(B)), namely: reduction in the intensities for bands in the region between 1600 cm^{-1} and 1731 cm^{-1}; a slight change in the shape of the broad band in the region between 3100 cm^{-1} and 3400 cm^{-1} after adsorption, the authors assumed interactions between the -COOH and OH-groups of bagasse and the sulfonic acid groups of CR. The maximum adsorption capacity of bagasse within the studied CR concentration range (100–500 mg L^{-1}) was found to be 38.2 mg g^{-1} [97]. Raymundo et al. [98] also reported the use of sugarcane bagasse in percolated columns to remove CR from both synthetic CR solution and an effluent solution enriched with CR [98]. The

results showed retention of approximately 64 % and 94 % CR from these two solutions, respectively. However, the maximum adsorption capacity was only 4.43 mg g^{-1} obtained with bagasse particles in the range of 1.19–4.76 mm. Besides, lower adsorption capacities (< 4.0 mg g^{-1}) were obtained with smaller bagasse particles (d$_p$ ≤ 1.19 mm) [98]. Commensurable adsorption capacities were also observed for coir pith activated carbon (q$_e$ 6.72 mg g^{-1}) by Namasivayam and Kavitha [20] and for *Psidium guajava* (q$_e$ 5.52 mg g^{-1}) by Naidu et al. [99] towards CR.

Carletto et al. [100] proved the applicability of untreated hazelnut shells as a potentially inexpensive biosorbent for CR removal from aqueous medium. The experimental results demonstrated 27.5 % removal of the azo dye for 48 h at C$_o$ 5,000 mg L^{-1}, corresponding to sorbent capacity q$_e$ 13.75 mg g^{-1}, and 37.5 % dye uptake for 48 h at C$_o$ 500 mg L^{-1}, corresponding to q$_e$ 1.87 mg g^{-1} [100].

Rehman et al. [101] studied the adsorption capacity of *Grewia asiatica* (Phalsa) leaves and *Raphanus sativus* (radish) peels for CR removal from aqueous media. The experimental results proved the efficiency of untreated and urea-modified Phalsa leaves. The latter exhibited the highest monolayer adsorption capacity (q$_m$ 0.566 mg g^{-1}) towards CR [101].

Venckatesh et al. [102] conducted an experimental study on the adsorption of CR using activated carbon prepared from *Punica granatum* (Pomegranate rind) by chemical activation with sulphuric acid [102]. The BET surface area of the activated carbon was 1075.6 m^2 g^{-1}, the pore volume - 0.185 cm^3 g^{-1}, the pore size - 250.2 Å, pH$_{PZC}$ - 6.2, and porosity - 89.22 %. SEM and X-ray diffraction studies proved the amorphous nature of the carbon. The examined *Punica granatum* activated carbon exhibited high potential for CR removal as the maximum adsorption capacity was 100.00 mg g^{-1} [102].

Palm kernel shell and palm kernel coat (PKC) are the major waste materials produced from the extraction of palm kernel oil and palm oil, respectively. In the study of Oladoja and Akinlabi [103] palm kernel coat was obtained immediately after the oil was extracted from it.

The residual oil on it was not allowed to biodegrade but was removed by saponification.

The ability of this sorbent to remediate water contaminated with CR was investigated in a batch mode. According to the proximate analyses the saponified PKC contained (% dry weight): proteins - 18.72 %; lipids - 3.72 %; ash - 1.37 %; fibers - 24.9 %; carbohydrates - 51.29 %; Ca - 0.5 %; Mg - 0.14 %; Na - 0.21 %; K - 0.05 %; P - 0.03 %; N - 3.00 %. The bulk density of the PKC was 497.28 kg m^{-3} [103].

Rajamohan [10] conducted a study subjected to utilization of water hyacinth roots through HCl acid modification as a potential adsorbent for CR removal from model aqueous solutions. The maximum reached adsorption capacity of this low-cost sorbent was q$_{max}$ 13.4646 mg g^{-1} [10].

TABLE III(A)
FTIR Spectrum Of Various Agricultural By-Products, Wastes
And Agro-Industrial Residues Applied As Adsorbents For CR Removal

Adsorbent	Bael shell carbon		Mahua oil cake		Jujuba seeds		Jute stick powder
FTIR spectra, cm⁻¹	-before ads.	- after ads.	-before ads.	-after ads.	-before ads.	-after ads.	-before ads.
-O-H	3387	3378 (pH 5.7) 3149 (pH 3)		3352.28	3416.19	3419.77	3406
N-H	3387	3378 (pH 5.7) 3149 (pH 3)		2341.58			
-CH		2834	2924 2850.79	2931.80	2925.69	2925.58	2900.7
-C=O	1689	1691 (pH 5.7) 1694 (pH 3)			1741.21 (aldehyde) 1649.93 (amide)	1735.60 (aldehyde) 1625.71 (amide)	1737..7
-NH₂	1590	1577 1587	1535.34	1531.48 1647.21	3761.36	3761.57	
-CH₂		1454.33	1436.90				
C-O-C		1041.56					
-C-N			1064.71				
C-O			1048.74		1043.16		
-N-O			1519.51		1510.16		
-C-H			1460.03		1458.87		
N-O			1378.5		1378.31		
C-Cl			604.66		609.08		
-SO₃	1256	1232 1211					
Ref.	[83]		[84]		[87]		[88]

TABLE III(B)
FTIR Spectrum Of Various Agricultural By-Products, Wastes
And Agro-Industrial Residues Applied As Adsorbents For CR Removal

Adsorbent	Nicols plant powder (ABPP)		Cashew nut shells (CNS)	Ball-milled sugarcane bagasse		Macauba palm cake		Pine cone powder
FTIR spectra, cm⁻¹	-before ads.	-after ads.	-before ads.	-before ads.	-after ads.	in natura (MCN) -before	thermally treated (MCT) ads.	-before ads.
-O-H	3294.53	3261.74	3399	3100-3400	3071	3400		3331.97
N-H	3294.53	32.61.74	3100-3500					
-CH	2843..68	2691.39	2854 (Ar)					2928.33
-C=O	1633.76	1627.97	1454	1731(carbonyl)				1602.37
-NH₂								
-CH₂			2925	2893			2928 2920	
-C-N	1060.8		1043.52	1232 (amine)				1263.56 (C-N stretching with amine)
C-O	1060.8		1043.52					1263.56 (C-O vibration of carboxylic acid)
C=C			3011			1646	1530 (Ar) 1644 1528 (Ar)	1602.37
P=O			1156					
P-OH			1035					
lignin Ar-ring C-O band stretching				1600	1514			
cellulose				1030				
N=N					1587			
C-C					1446 (Ar)	1041	1041	
S-O					1354			
Ref.	[89]		[91]	[97]		[13]		[57]

Water hyacinth is an aquatic plant found widely in India, listed as one of the most productive plants on earth and considered as one of the world's worst aquatic plants. Due to vegetative reproduction and extremely high growth rate, water hyacinth has attracted the attention of scientists also as a substrate for compost or biogas production, as well as an efficient fertilizer for the nutrient deficient soils and feed for livestock [10],[104].

The elemental composition of Macauba cake *in natura* (MCN) applied by Vieira et al. [13] for Methylene blue and CR adsorption, was C 50.93 %, O 40.68 %, H 6.59 %, N 1.60 % and S 0.197 %, indicating that the adsorbent material was rich in oxygen but contained only low levels of sulfur [13]. The FTIR spectral details of MCN and Macauba cake thermally treated (MCT), presented in Table III(B) indicated that Macauba palm cake contained functional entities, such as phenolic OH−groups, that can interact with dyes functional groups. The SEM analysis showed the fibrous structure of both biosorbents employed in the work. MCN and MCT presented negative surface charges (from -7 to -25 mV) throughout the pH range studied (2.0–11.0) signifying that both adsorbents would exhibit a great affinity for cations. The negative charge present on the surface of lignocellulosic materials is associated with acidic entities such as −COOH and phenolic OH−groups. Interestingly, however, at any particular pH the charge on the surface of MCT was less negative than that of MCN suggesting that thermal treatment degraded a small proportion of these acidic groups [13].

Sunflower stalks were studied as adsorbents for basic and direct dyes removal from aqueous solutions. The surface area of the material was 1.2054 m^2 g^{-1} and the adsorption capacity of the adsorbent towards CR - 37.78 mg g^{-1}. The authors suggested that since sunflower stalks consist of cellulose, it was the polyol structure of cellulose-based materials that exhibited relatively strong chemical adsorption of cations such as metal ions and organic bases, as well as physical adsorption of other acidic and anionic compounds. They stated also that the coulombic forces between dye species and negatively charged cellulose in water were the major interactions which affected the adsorption of dyes on the biomaterials studied [105]. Shi et al. [106] obtained 4.5 times increase in the adsorption capacity when sunflower stalk biomass was chemically grafted with quaternary ammonium groups. The maximum capacity of the modified adsorbent to CR was 191.0 mg g^{-1}. Rashwan and Girgis [107] established enhanced adsorption capacity of phosphoric acid treated rice straw (54.00 mg g^{-1}) and water hyacinth biomass (154.00 mg g^{-1}) towards CR after pyrolysis of the biomaterials.

Pine cone a natural, low-cost agricultural by-product in Australia was studied for its potential application as an adsorbent for CR removal in its raw and HCl-modified form. Pine cone is composed of epidermal and sclerenchyma cells which contain cellulose, hemicelluloses, lignin, rosin, and tannins in their cell walls which contain polar functional groups such as: alcoholic, aldehyde, ketone, carboxylic, phenolic, etc. [53],[108]. The FTIR spectra of raw (Table III(B)) and acid modified pine cone powder exhibited similar peaks with slight differences in the intensities of the band at 3331.97 cm^{-1}, the peak at 2928.33 cm^{-1} and 1602.37 cm^{-1}, indicating unbounded −OH, aliphatic C−H group and C=O stretch [109]. The availability of pores and the internal surface was clearly displayed in the SEM pictures of the pine cone biomass before adsorption and the coverage of the surface and the pores by the adsorbed CR molecules. The specific surface area of raw pine cone biomass was 0.0993 m^2 g^{-1}, and that of acid-treated pine cone - 0.122 m^2 g^{-1}. The pH_{PZC} of pine cone particles in aqueous solution was 4.4 and the negative zeta potential increased with increasing alkaline solution pH. Surface modification reduced the pH_{PZC} of the activated pine cone to 3.06 [57].

IV. Adsorption Mechanism and Modelling

IV.1. Effect of pH and Sorbate/Sorbent Interactions

pH is one of the basic parameters that have to be accounted when analyzing the adsorption behaviour of sorbate-sorbent systems and outlining the mechanism of the process as it affects both aqueous chemistry and the surface binding-sites of the adsorbents [96]. Adsorbate solution pH affects the adsorption capacity of the adsorbent through modification of the state of ionization of the binding groups, either increasing or decreasing the competition between the protonated species and adsorbate molecules for the active sites. Therefore, the optimal pH depends on the chemical nature of the adsorbate and adsorbent. Hence, to intensify adsorption, preliminary tests have to be performed to determine the most favourable pH for the isotherms construction [13]

At pH below the isoelectric point, a dye exists predominantly in the molecular form, while above the isoelectric point it exists with a higher proportion in its dissociated form. The isoelectric point of CR is 3, thus CR would be negatively charged at pH range 5.0–10.0 [83],[97]. As outlined in Section III, the activity of an adsorbent is due to the presence of different functional groups: carboxylic (−COOH), sulfonyl (−S−O), amine (−NH$_2$), hydroxyl (−OH), etc. At higher pH (basic pH), these groups become anionic in nature (carboxilate, COO−) and are not suitable for the adsorption of negatively charged dye molecules due to interionic repulsion between similarly charged particles [84]. The adsorption of an anionic dye generally decreases with an increase in pH, and this phenomenon is associated not only with the negative charge on the surface of the adsorbent but also with excess OH⁻ ions in the solution that compete for the adsorption sites [13],[110]

The adsorption of CR on bael shell carbon (BSC) was studied in the pH range of 3–9 and maximum adsorption (E 92 %) was observed at pH 3. The maximum adsorption onto BSC at lower pH may be due to the

greater positive charge on the adsorbent surface. According to Ahmad and Kumar [83] the adsorption process could be explained via van der Waals forces, electrostatic, H−bonding and hydrophobic–hydrophobic interactions. The authors explained their role as follows: (i) in acidic medium, the protonation of –OH and –COOH groups at the BSC surface occurred (since pH_{PZC} of the adsorbent is 6.28, below which the adsorbent surface is positive). Generally, the carboxyl groups presented a pKa value between 3.0 and 5.0. At pH < pKa, carboxylate groups carry positive charge resulting in electrostatic interaction between negatively charged SO_3^- groups and the positively charged adsorbent surface; (ii) H-bonding between oxygen and nitrogen containing functional groups of CR and BSC surface; (iii) Hydrophobic–hydrophobic interaction between hydrophobic parts of CR and BSC; (iv) in basic medium, the carboxylic groups of BSC were expected to completely ionize. Therefore, electrostatic repulsion between anionic CR and anionic BSC surface which lowers the adsorption capacity could be expected. Ahmad and Kumar [88] and Wang and Wang [24] reported that −NH$_2$, –N=N–, –HN–N and –SO$_3$ groups of CR were involved in the adsorption. According to Chatterjee et al. [29] the three-dimensional energy minimized structure of CR molecule drawn with Chem Office 3D ultra software appeared to be flat [29]. Thus, attachment of the dye molecule on the surface of chitosan beads is of flat layer type. Hence, there is a possibility of hydrogen bond formation between some of the molecular components of CR such as N, S, O, benzene ring and CH$_2$OH– groups of the chitosan molecule. At pH > 6.4, the surface charge of chitosan beads is negative which hindered the adsorption by electrostatic force of repulsion between the negatively charged dye molecule and adsorbent (chitosan hydrobeads); but appreciable amount of adsorption in this pH range suggested strong involvement of physical forces such as hydrogen bonding, van der Waals force, etc. in the adsorption process [29].

Mishra et al. [84] established that the extent of dye adsorption on the surface of Mahua oil cake (MOC) was low at basic pH. At acidic pH, CR molecules existed as cations and the active sites of MOC remained carboxylic (–COOH). Cationic dye molecules got attached on the surface of MOC by replacing the H$^+$ ion of the carboxylic group. It was observed that at pH 2.0, CR uptake was 8.2 mg g^{-1} at initial dye concentration C$_o$ 50 mg L^{-1}. On the other hand, CR adsorption decreased with an increase in pH up to 8 [84].

The investigations of Sarkar and Bandyopadhyay [86] established that CR as an anionic dye was adsorbed onto the surface of rice husk ash (RHA) more effectively at lower pH values since the adsorbent surface attained acidity at lower pH values (Eq. (1)):

$$\text{Adsorbent–OH} + H^+ \rightarrow \text{Adsorbent–OH}_2^+ \qquad (1)$$

The optimum solution pH was observed to be 4.0 for CR dye and the optimum adsorbent mass - 80.0 g L^{-1} [86]. Han et al. [32] assumed two possible mechanisms of CR adsorption on unmodified rice husk in a fixed bed column: a) electrostatic interaction between the protonated groups of the adsorbent and the acid dye and/or b) chemical reaction between the adsorbate and the adsorbent. At pH 3, a significantly high electrostatic attraction existed between the positively charged surface of the adsorbent and the anionic dye molecules which influenced the mode of the breakthrough curves - they shifted from left to right with pH decrease, which indicated higher efficiency of the adsorption process at lower pH values [32].

The investigations of Somasekhara Reddy et al. [111] also established an inverse relationship between pH and CR uptake by tamarind fruit shells: increasing the pH from 5.5 to 12 led to a decrease in the dye percent removal from 83 to 68 %. The extent of CR adsorption on Jujuba seeds, however, was not affected over a pH range of 5–12 and the maximum dye uptake was achieved at pH ≤ 2 [87]. The authors established that for both systems studied, namely CR/tamarind fruit shells and CR/Jujuba seeds, the final pH (after adsorption) was higher than the initial pH (after desorption) of the solution with no dye, which could be attributed to the consumption of H$^+$ ions during the desorption of alkali metal ions present in the adsorbent and a probable exchange of H$^+$ ions with alkali metals as well as with dye molecules [87],[111]. Namasivayam and Kavitha [20] observed maximum extent of CR uptake by coir pith activated carbon (E 70 % at C$_o$ 20 mg L^{-1}; E 50 % at C$_o$ 40 mg L^{-1}) at pH 2. The capacity of the adsorbent decreased in the range pH 2–4 and remained almost constant at pH up to 10 [20].

Panda et al. [88] found out that the extent of CR adsorption on Jute stick powder (JSP) remained nearly constant (q$_e$ 4.6 mg g^{-1}) in the pH range of 7.0–10.0. Considering that JSP is a heterogeneous polymer of cellulose, hemicellulose and lignin [112], thus containing various functional groups, such as carboxyl and hydroxyl, etc., the adsorption of the dye on JSP might be attributed to weak electrostatic sorbate-sorbent interactions [88]. Patil and Shrivastava [89] determined that the highest percent CR uptake (80.5 %) by *Alternanthera bettzichiana* plant powder (ABPP) was obtained at pH 5. The maximum removal of CR on cashew nut shells (CNS) (> 93 %) was observed at pH ≤ 3 [91] and on Guava (*Psidium Guajava*) leaf powder - at pH 1 [99].

Approximately 100 % removal efficiency of CR by cattail root was achieved at pH ~ 2.5, which was attributed to the very low solubility of CR at pH < 2.5 [92]. According to the study of Annadurai et al. [96], the adsorption capacity of banana peels towards CR reached a maximum value (q$_{max}$ 11.2 mg g^{-1}) at pH 6–7, but decreased at 6 > pH > 7. In the case of orange peels, however, the maximum adsorption capacity (q$_{max}$ 7.9 mg

g^{-1}) was achieved at pH ~ 8, while at pH > 7 CR concentration curve reached a plateau. Annadurai et al. [96] measured also the zeta potentials of banana and orange peels as a function of pH: at pH 2.0 - 8.0 the p$_{PZC}$ declined from −8.2 to −62.4 mV and from −3.2 to −44.5 mV, respectively. The authors stated that the sharper change in the zeta potential values for banana peel than orange peel may explain their different pH trends during CR adsorption [96]. The investigations of Namasivayam and Kanchana [113] established 92 % uptake (q$_e$ ~ 5.00 mg g^{-1}) of the azo dye by waste banana pith at pH 2 and no considerable pH dependence of the adsorption process in the pH range 2–11 [113]. The study of Zhang et al. [97] ascertained 93.4 % CR removal by ball-milled sugarcane bagasse at pH 5, dropping to 84.7 % at pH 10. At pH 5.0, the charge of bagasse will be zero and at pH > 5.0 bagasse will be negatively charged. Thus, the decrease in CR removal with increasing pH, in the present study, could be attributed to reduced electrostatic attractions between CR molecules and bagasse [97]. Rehman et al. [101] observed 87.26 % CR removal by *Raphanus sativus* peels at pH 3.0, 96.35 % - by *Grewia asiatica* leaves at pH 7.0 and 95.6 % - by activated charcoal at pH 2.0. The results of Abbas et al. [114] and Jayrajan et al. [115] established 97.266 % CR removal by *Raphanus sativus* peels at optimum pH 10.0, and q$_{max}$ 29.1 mg g^{-1} of pomelo fruit peel nano-porous sorbent at optimum pH 8.73, respectively, which were in contradiction with the above stated results, although the Raddish peels in both studies were supplied from Pakistan and the methodologies for adsorbent preparation were similar [114],[115].

Nagda and Ghole [116] studied the adsorption of CR on tendu leaf refuse (TLR) and hydrogen peroxide treated TLR (TLR-H2O2). Tendu leaf *Diospyros melanoxylon* is the second largest forest product in India after timber and is exclusively used in making local cigarette called Bidi. The optimum initial pH for CR biosorption was 6.5 for both adsorbents. An approximately constant extent of dye uptake (70 - 75 %) in the range pH 5–10 was established [116]. Similar results were reported by Rajamohan [10] during CR adsorption on HCl acid-activated water hyacinth roots. The dye uptake was found to be optimal at pH 6.0 with q$_{max}$ 46.15 mg g^{-1}.

In the pH ranges 2.0–5.0 and 7.0–10.1 a decreasing trend in q$_{max}$ values was observed [10]. Vieira et al. [13] reported that the adsorption of CR on MCN and MCT was favoured at pH 6.5 in comparison to pH 10. The efficiency of the adsorbent MCN (54 %) was higher than that of MCT (34 %). The adsorption of CR was not investigated at pH 2.0, because at this pH the colour of the solution changed and the wavelength of maximum absorption was altered [13].

Dawood and Sen [57] stated that the change of CR solution initial pH from 3.55 to 10.95 exerted negligible effect on λ$_{max}$ values. It was found that the amount of dye adsorbed on the raw adsorbent increased from 2.88 mg

g^{-1} (E 5.75 %) to 31.9 mg g^{-1} (E 60.5 %) due to pH change from 10.95 to 3.55. Similarly, it was established that the amount of CR adsorbed by the acid modified agricultural material increased from 8.34 mg g^{-1} (E 16.25 %) to 39.48 mg g^{-1} (E 79.25 %) with pH change from 7.45 to 3.61 [57].

Based on these observations, a clear and general conclusion regarding the optimum pH range for CR adsorption on the lignocellulosic materials reviewed could not be defined due to contradictious literature results.

The observed deviations of the pH effect on CR adsorption, however, could be explained by the consistent and adequate comments of Qi et al. [117] subjected to the detection of an obvious error in determining the maximum absorption wavelength as a function of pH, and the subsequent calculation of CR solution concentrations found in a number of articles.

The laboratory spectrophotometric experiments of this scientific team established that for CR initial concentration 50 mg L^{-1} at pH 2.18–3.16 λ$_{max}$ was 576 nm; at pH 3.86 - λ$_{max}$ was 567 nm, and at pH ≥ 4.71 - λ$_{max}$ was 496 nm. Thus for calculating the accurate solution concentration, pH-specific standard calibration curves should be generated at these maximum absorption wavelengths and used in its respective pH range (Fig. 2) [117].
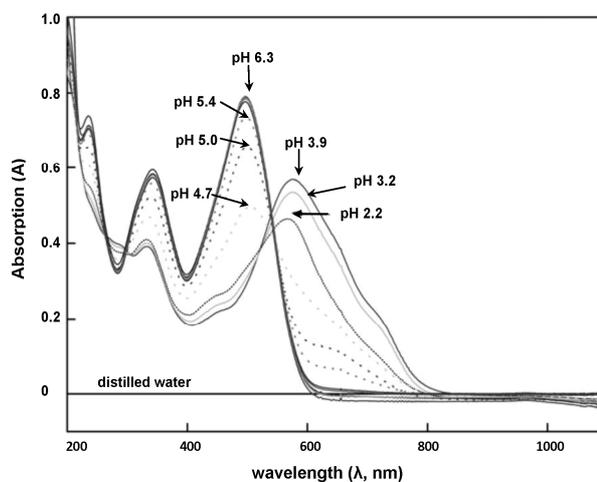

Fig. 2. UV/VIS spectra of CR solution at different pH adapted from [117]

In the context of the above stated, the probable physical, physicochemical and ionic interactions between the surface functional groups of various lignocellulosic adsorbents and CR macromolecules during adsorption are summarized in Figs. 3.

IV.2. Effect of Ionic Strength

Hu et al. [92] stated that since NaCl is often used as a stimulator in dying processes and ionic strength affects the activity coefficients for OH$^-$, H$_3$O$^+$ and specifically

absorbable ions, the ionic strength of NaCl may have impact on the removal of dyes from wastewater.

(a)

(b)
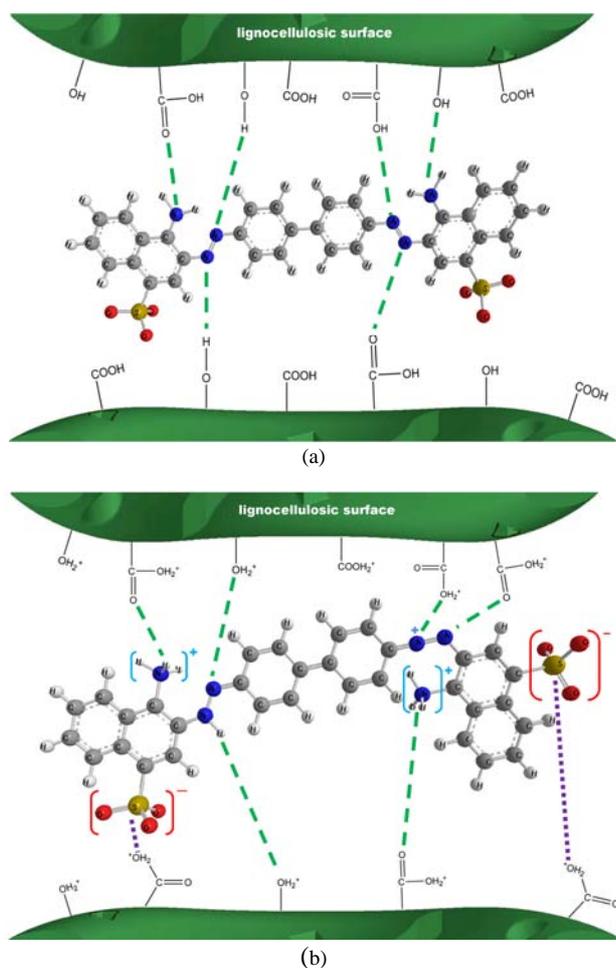
Figs. 3. Mechanism of CR adsorption on lignocellulosic materials at: (a) pH 6.0; (b) pH 3.0. Adapted from [29], [83]

According to Han et al. [32] the presence of electrolytes in solution reduced repulsive forces between CR molecules and the functional groups on the surface of rice husk due to screening effect of the superficial charge. When 0.1 mol L^{-1} of NaCl was added to the single component CR solution, the anionic exchange capacity was increased, probably due to a decrease in the repulsive forces. Thus, rice husk could be used to remove CR from aqueous solutions with a higher salt concentration [32]. Similar tendency was observed by Hu et al. [92] who established a strong impact of NaCl concentrations on the extent of CR removal by cattail root at C_o 50 mg L^{-1}, temperature 20°C, and pH 7.0±0.3.

The dye uptake reached 99 % with an increase in the ionic strength of NaCl from 0 to 1 mol L^{-1}. The latter dependence could be attributed to a direct relationship between the increase in the ionic strength and the positive charge of the surface leading to increased electrostatic interaction between the dye and cattail root [92].

IV.3. Equilibrium Studies

Studies in finite batch mode under agitation assume significant importance for yielding equilibrium and kinetic data [86]. The mode of adsorption isotherms is fundamental for the determination of the maximum capacity of the adsorbent, providing a panorama of the course of the system studied, indicating adsorbent efficiency and allowing estimation of the economic viability of the sorbent commercial applications for the specified solute [91]. In fact, adsorptive mass transfer is governed by the external liquid film resistance and the pore diffusion resistance in series [86].

According to the investigations of Ahmad and Kumar [83] the maximum monolayer adsorption capacity of bael shell carbon (BSC) was found to be 98.03 mg g^{-1}. The values of the correlation coefficients of Langmuir, Freundlich and Temkin models were determined as R^2 0.9679, 0.972 and 0.9399, respectively. This revealed that the data were better described by the Freundlich model indicating heterogeneous and multilayer adsorption [83]. The adsorption studies of Sarkar and Bandyopadhyay [89] and Naidu et al. [99] regarding CR adsorption on RHA and Guava (*Psidium Guajava*) leaf powder, respectively, established that the Langmuir model described satisfactory the equilibrium behaviour of the azo dye based on the high values of the correlation coefficients (R^2 0.97 for RHA) [89],[99]. The equilibrium data of CR adsorption on Indian Jujuba seeds fitted well to the Langmuir model, with a maximum adsorption capacity q_{max} 55.56 mg g^{-1}. The Langmuir, Freundlich and general isotherm equations were suitable for modelling the experimental data of CR on IJS (*Z. maruritiana*) based on the high values of the calculated correlation coefficients ($R^2 > 0.987$) [87]. The R_L value for the adsorption of CR on IJS was 0.0124, indicating that the investigated adsorption process was favorable [87]. The experimental equilibrium data for CR adsorption on jute stick powder (JSP) fitted well the Langmuir isotherm model with R^2 0.999, supporting monolayer coverage of the adsorbate on the surface of the adsorbent [88]. The calculated theoretical monolayer saturation capacity of JSP was q_m 35.7 mg g^{-1} and, the value of R_L 0.049 indicated a favourable adsorption process [88]. According to the study of Patil and Shrivastava [89] the q_{max} for ABPP towards CR was 14.66 mg g^{-1}. The determined R_L value of 0.2512, at C_o 20 mg L^{-1} CR, proved the favourable mode of the adsorption isotherm. The experimental data were correlated reasonably well by both the Langmuir (R^2 0.9922) and Freundlich (R^2 0.9960) equilibrium models [89]. The sorption process of CR on Neem leaf powder was also favourable and in conformity with both the Langmuir and Freundlich isotherms [90]. Kumar et al. [91] conisedered the Langmuir, Freundlich, Redlich–Peterson, Koble–Corrigan, Sips, Toth, Temkin and Dubinin–Radushkevich equations in order to adapt an adequate model that can reproduce the experimental equilibrium results of CR adsorption on CNS [91]. Based

on the corresponding R^2 values and the mode of the experimental and model isotherms, the applicability of the applied mathematical equations followed the order: Redlich–Peterson (R^2 0.999) > Toth (R^2 0.999) > Koble–Corrigan (R^2 0.999) > Sips (R^2 0.999) > Freundlich (R^2 0.998) > Langmuir (R^2 0.981) > Temkin (R^2 0.976) > Dubinin–Radushkevich (R^2 0.801) [96]. The q_{max} of cattail root towards CR at 20, 30 and 40°C were 38.79, 34.59 and 30.61 mg g^{-1}, respectively, indicating that temperature increase induced lower maximum adsorption capacity [92]. The R_L values (0.0260 - 0.4994, i.e. $R_L <$ 1) revealed that cattail root was a favourable adsorbent for CR removal.

The equilibrium experimental data fitted well to the Langmuir model ($R^2 > 0.98$) [92]. The investigations of Annadurai et al. [96] revealed that the equilibrium adsorption behavior of CR on banana and orange peels was better approximated with the Freundlich model based on the higher values of the calculated correlation coefficients (R^2 0.9589 and 0.9820, respectively) compared to the Langmuir equation (R^2 0.9480 and 0.9739, respectively). Besides, banana peels characterized with a higher value of q_m 18.2 mg g^{-1} towards the azo dye compared to that of orange peels (q_m 14.0 mg g^{-1}) [96]. CR adsorption on ball-milled sugarcane bagasse [97] and pine cone powder [57] fitted the Freundlich isotherm very well (R^2 0.9971 - ball-milled sugarcane bagasse; R^2 0.95 - pine cone powder) indicating that the adsorption processes occurred on heterogeneous surfaces.

The investigations of Viera et al. [13] demonstrated that the Langmuir and Sips equations provided the best models for the adsorption of CR onto MCN and MCT. Consequently, both monolayer adsorption and heterogeneous energetic distribution of active sites on the surface of the adsorbents were possible. The maximum adsorption capacity of MCN (q_{max} 32.00 mg g^{-1}) was larger than that of MCT (20.30 mg g^{-1}) towards CR [13].

The experimental equilibrium data for CR adsorption on TLR and TLR-H2O2 obeyed both Freundlich and Langmuir models exhibiting heterogeneous surface conditions and monolayer adsorption [116]. The monolayer adsorption capacity of raw biomass (TLR) was q_m 46.96 mg g^{-1}. According to the authors H_2O_2 used for the pretreatment of tendu biomass as an oxidizing agent, produced oxidative delignification and increased the positive valance state of the molecule by removal of one or more electrons from an atom or ion from the adsorbent surface.

The q_{max} for TLR was 46.95 mg g^{-1}, which was enhanced by 2.8 times after H_2O_2-treatment to 134.4 mg g^{-1} [116]. Rajamohan [10] analyzed the experimental equilibrium data for CR adsorption on acid activated water hyacinth roots by applying the Langmuir, Freundlich and Redlich-Peterson isotherm equations.

The results obtained proved that Redlich–Peterson isotherm (R^2 0.9948) best fitted the experimental isotherm throughout the entire concentration range [10].

The equilibrium adsorption behavior of CR on coir pith activated carbon was successfully modelled by the Langmuir model (R^2 0.9958), while the Freundlich equation gave satisfactory approximation only in the low concentration range (R^2 0.9941) [20].

IV.4.   Kinetic and Mass Transfer Studies

Molecular shape and size, on the one hand, and adsorbent pore size and pore size distribution, on the other are the prime parameters defining the possibility for the accomplishment of intra-particle diffusion processes during dye molecules adsorption. The software package CS Chem 3D ultra was used by Chatterjee et al. [29] to calculate the Connolly molecular surface area of CR molecule, which gives a fairly accurate prediction of the area occupied by spatial orientation of various functional groups and structures of a molecule and enabling the estimation of its ability to diffuse through the porous networks of the studied adsorbents. The CR molecular surface area was calculated as 557.6 $Å^2$ predicting large dimensions of the dye molecule [29].

The pseudo-second-order model fitted well the experimental kinetic data for CR sorption on bael shell carbon at pH 5.7, 7 and 8, whereas at pH 9.5, the pseudo-first-order model was the rate-limiting step [85]. Sarkar and Bandyopadhyay [86] applied the shrinking core model, widely used for modelling of the adsorption behaviour of fluid–solid non-catalytic reactive systems, to characterize the adsorption of Methylene Blue (MB) and CR dyes in the aqueous phase onto rice husk ash (RHA). The model predictions agreed reasonably well with the experimental data, with a maximum standard deviation (SD) of 0.0347 for MB and 0.0599 for CR. The values of pore diffusivity of MB and CR dye molecules in RHA were also determined - 1.12×10^{-9} and 8.71×10^{-10} m^2 s^{-1}, respectively. These results demonstrated that Methylene blue dye molecules diffused faster than CR dye molecules resulting in better removal of MB. The findings of this work could be useful in the design and simulation of a packed bed adsorption column intended to be applied in practice [86]. The pseudo-second-order kinetic model provided a better correlation ($R^2 > 0.9947$) for the adsorption of CR on Indian Jujuba seeds at different initial CR concentrations compared to the pseudo first-order model [87]. The experimental kinetic results were also analyzed by the intraparticle diffusion model (Weber and Moris model) to identify the diffusion mechanism.

The plots of t/q_t against t were not linear over the entire time range implying that more than one process affected the adsorption. Besides, three linear regions were detected on the plot of q_t vs $t^{0.5}$: one at the beginning of the adsorption process representing the rapid surface loading, followed by the second - representing pore diffusion, and the third - depicting the equilibrium state. The calculated values of the intraparticle coefficient (k_i) for first linear region

increased slightly from 0.534 to 2.36 mg g^{-1} min$^{-0.5}$ with an increase of CR initial concentration from 25 to 75 mg L^{-1} [87].

Linearity with a high R^2 value (0.999) indicated that the sorption of CR on jute stick powder followed a pseudo second-order rate model [88]. Besides, the biphasic nature of t/q$_t$ curves indicated that the process occurred in two steps: initial steep portion attributed to the transport of dye molecules from the bulk solution to the surface of the adsorbent and the linear portion - to the binding of dye molecules on the active adsorbent sites [88]. The high values R^2 > 0.9926 and the commensurable values of the experimental (q$_e^{exp}$ 4.00 mg g^{-1} at C$_o$ 10.0 mg L^{-1}; q$_e^{exp}$ 10.05 mg g^{-1} at C$_o$ 30.0 mg L^{-1}) and model (q$_{e2}$ 4.44 mg g^{-1} at C$_o$ 10.0 mg L^{-1}; q$_{e2}$ 10.00 mg g^{-1} at C$_o$ 30.0 mg L^{-1}) adsorption capacities indicated the applicability of the pseudo-second-order model to the experimental data for CR sorption on ABPP [89].

The % CR removal by CNS increased from 56.33 to 99.34 % for an increase in the adsorbent dose from 5 to 30 g L^{-1} because of the concentration gradient between CR concentration in the solution and the CR concentration on the sorbent surface. The experimentally obtained q$_{max}$ was 4.261 mg g^{-1} at C$_o$ 100 mg L^{-1} [91].

The pseudo-second-order kinetic model agreed very well with the adsorption behavior of CR onto CNS [96], coir pith activated carbon [20] and Guava (*Psidium Guajava*) leaf powder [99] for different initial CR concentrations over the whole range studied.

The results related to the kinetic behaviour during CR adsorption on MCN and MCT revealed that the experimental data could best be described as a pseudo second order reaction controlled by the interaction between the dye molecules and the functional groups distributed on the surface of MCN (R^2 0.9874) and MCT (R^2 0.9644) [13].

Adsorption kinetics analysis indicated that the pseudo-second-order equation fitted very well also to the experimental results for CR adsorption on cattail root (R^2 > 0.99) [92] and Neem leaf powder [90].

The intraparticle diffusion model, however, showed that more than one diffusion mechanism was responsible for CR adsorption on both biosorbents [90],[92]. The intraparticle diffusion of CR molecules within the banana and orange peel particles was found to be the rate controlling stage during CR adsorption after 20 min of contact [96].

The experimental kinetic curves of CR sorption on ball-milled sugarcane bagasse obeyed the pseudo-second order equation [97]. The intraparticle diffusion model described very well the adsorption behavior of the studied system with sorbent surface area in the range of 0.58–0.66 m^2 g^{-1}, whereas the process was controlled by multi-adsorption stages with bagasse surface area in the range of 1.31–1.82 m^2 g^{-1} [97]. The adsorption of CR by TLR, TLR-H2O2 [116] and PKC [103] followed pseudo-second order kinetic mechanism, with extremely

high correlation coefficients (R^2 > 0.999) and negligible values of the Chi square error χ^2 (< 0.0009).

Besides, the intraparticle diffusion was found to be the rate-controlling mechanism during CR removal by palm kernel coat (PKC) at low dye concentrations, while at high concentrations film diffusion was the main rate-controlling step [103].

IV.5. Thermodynamic Studies

The determination of the basic thermodynamic parameters: enthalpy of adsorption (ΔH◦), Gibb's free energy of adsorption (ΔG^o) and entropy of adsorption (ΔS^o), is important as it allows to estimate if the process is favourable or not from thermodynamic point of view, to assess the spontaneity of the system and to ascertain the exothermic or endothermic nature of the process. An adsorption process is generally considered as physical if ΔH◦ < 84 kJ mol^{-1} and as chemical when ΔH◦ lies between 84 and 420 kJ mol^{-1} [83]. The negative ΔH◦ value reveals that the adsorption process is exothermic [30]. The negative ΔS◦ indicates a decrease in randomness at the solid/solution interface [97].

The adsorption capacity of bael shell carbon (BSC) towards CR was found to increase from 40 to 46 mg g^{-1} with increase in temperature [83].

Ahmad and Kumar [83] explained the latter by the fact that an increase in temperature may increase the rate of diffusion of the adsorbate molecules across the external boundary layer and in the internal pores of the adsorbent particle and may decrease the viscosity of the solution. The negative ΔG◦ values: –3.986, –4.46 and –5.781 kJ mol^{-1} at 25, 40 and 55°C, respectively, indicated the spontaneous nature of CR adsorption on BSC.

The positive ΔH◦ value (13.613 kJ mol^{-1}) confirmed the endothermic and physical nature of CR adsorption, while the positive value of ΔS◦ (58.8 J mol^{-1} K^{-1}) reflected the affinity of CR towards BSC [83].

The study of Viera et al. [13] demonstrated analogous thermodynamic behavior during CR adsorption on MCN and MCT. The values of the thermodynamic parameters were: ΔG◦ -21.43 ÷ -25.37 kJ mol^{-1}; ΔH◦ 18.31 kJ mol^{-1} (for MCN) and 35.83 kJ mol^{-1} (for MCT); ΔS◦ 135.77 J mol^{-1} K^{-1} for MCN and 192.15 J mol^{-1} K^{-1} for MCT [13].

The negative value of ΔH^o (–8.339 kJ mol^{-1}) for CR adsorption on Mahua oil cake (MOC) indicated that the reaction was exothermic [84]. The uptake of CR on IJS increased from 79.68 % to 99.82 % with increase in temperature from 30 to 60°C [87].

The latter was mainly due to the increased surface activity suggesting that adsorption between CR and IJS (*Z. maruritiana*) was endothermic. The positive value of ΔS◦ 0.0579 kJ mol^{-1}K^{-1} revealed increased randomness at the solid/ solution interface and corresponded to an increase in the degree of freedom of the adsorbed species.
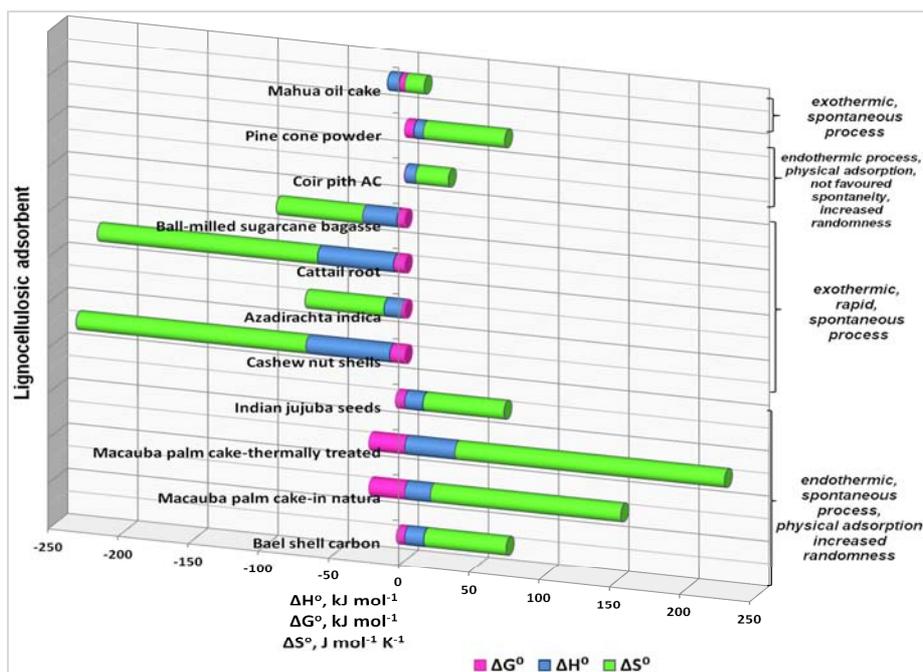
Fig. 4. Thermodynamic nature of CR adsorption on various lignocellulosic materials. Graphically presented data adapted from [13],[20],[57],[83], [84],[87],[90]-[92],[97]

Thus, CR adsorption on IJS was thermodynamically favourable [87]. The negative ΔG^o values (-10.576 ÷ -3.317 kJ mol^{-1}) indicated the feasibility and the spontaneous nature of CR adsorption on CNS; the negative ΔH^o values (-59.567 ÷ -15.844 kJ mol^{-1}) suggested the exothermic nature of adsorption and the negative ΔS^o values (-163.976 ÷ - 37.873 J mol^{-1} K^{-1}) described the randomness at the CNS-solution interface during the adsorption process [91]. Bhattacharyya and Sharma [90] proved that CR sorption on *Azadirachta indica* leaf powder was exothermic with an average heat of adsorption of −12.75 kJ mol^{-1}. The spontaneity of the sorption process was confirmed by the favourable values of ΔG^o −1.09 to −1.81 kJ mol^{-1}, and ΔS^o −18.97 to −56.32 J mol^{-1} K^{-1} [90].

The values of $\Delta G \circ$ (−7.871 and −4.702 kJ mol^{-1}) indicated spontaneous CR adsorption by cattail root, more favourable at low temperature. The negative value of $\Delta H \circ$ (−54.116 kJ mol^{-1}) revealed that the process was exothermic and likely to be dominated by physical processes in nature. The negative value of $\Delta S \circ$ (−0.157 kJ mol^{-1}K^{-1}) suggested a slight decrease in randomness at the solid/solution interface with increasing temperature [92]. Reduced CR removal by ball-milled sugarcane bagasse from 89.9 % to 83.0 % with temperature increase from 30°C to 50°C was ascertained by Zhang et al. [97]. The ΔH^o was −24.25 kJ mol^{-1} indicating that CR adsorption on bagasse is probably an exothermic physical process. The negative values of ΔG^o obtained at 30, 40 and 50°C indicated that the process is spontaneous in nature, and the shift of $\Delta G \circ$ from −5.5 to −4.2 kJ mol^{-1} with decreasing the temperature was indicative of a rapid and more spontaneous adsorption at the lower temperature. The negative $\Delta S \circ$ value (-61.59 J mol^{-1} K^{-1}) indicated that no marked changes occurred in the internal structure of bagasse through the adsorption process [97].

The positive values of ΔH^o (7.705 kJ mol^{-1}) confirmed the endothermic nature of CR adsorption on coir pith activated carbon [20]. The negative value of ΔG^o at 60°C indicated spontaneous adsorption, while the positive ΔG^o values (0.487–0.144 kJ mol^{-1}) in the temperature interval 35–50°C indicated that spontaneity was not favoured at low temperatures. The positive values of ΔS^o (23.549 J mol^{-1} K^{-1}) suggested increased randomness at the solid/solution interface during the dye adsorption on coir pith carbon [20]. The thermodynamic investigations of Dawood and Sen [57], however, demonstrated quite different behavior of the system CR-pine cone powder, as the values of the three studied parameters were positive, indicating endothermic nature of the process, increased randomness at the solid-solution interface and unfavoured spontaneity. The comparative analyses categorized the lignocellulosic adsorbents into four groups according to their thermodynamic adsorption behaviour presented in Fig. 4.

IV.6. Dynamic Studies

Adsorption dynamics acquaintance and modelling are essential because they provide valuable information on some practical aspects such as sorbent capacity and prediction of the time necessary for the effective operation of a fixed-bed column. At the same time they assist in making more detailed conclusions about the mechanism of the process. Some of the mathematical correlations for adsorption in fixed-bed columns are

based on the assumption of one mass transfer resistance, while others consider the influence of more mechanisms, as well as the effect of axial dispersion [118]. Han et al. [32] conducted a continuous fixed bed study by using rice husk as a biosorbent for the removal of CR from aqueous solution.

The experimental data confirmed that the breakthrough curves were dependent on flow rate, initial dye concentration and bed depth. Thomas, Adams–Bohart, and Yoon–Nelson models were applied to the experimental data to predict the breakthrough curves using non-linear regression analyses and to determine the characteristic parameters of the fixed-bed column useful for process design. The Bed Depth-Service Time (BDST) model was used to express the effect of bed depth on the mode of the breakthrough curves. The results showed that Thomas model was found suitable for the normal description of the experimental breakthrough curves, while Adams–Bohart model described satisfactory only the initial part of the experimental curve (up to C_t/C_o 0.5). The high values of R^2 ranging from 0.980 to 0.998 ascertained that the data were in good agreement with the BDST model [32].

V. Desorption Studies

Desorption studies help to elucidate the mechanism of adsorption and recovery of the adsorbate and adsorbent. Regeneration of adsorbent makes the treatment process economical.

According to Mall et al. [119] if the dye adsorbed on the adsorbent can be desorbed by water, it can be assumed that the attachment of the dye onto the adsorbent is due to weak bonds. If strong acid or strong base can desorb the dye, the attachment of the dye to the sorbent is regarded as ion exchange. If organic acid can desorb the dye, the adsorption of the dye onto the adsorbent is accepted as chemisorption [119]. The correlation between pH and the amount of adsorbate desorbed is just converse to that between pH and the percent uptake during adsorption.

The latter dependence was sustained by the investigations of Reddy et al. [87] and Dawood and Sen [57] subjected to CR removal by Jujuba seeds and pine cone powder, respectively. The desorption results of Reddy [87] established decreased percent of CR desorption from Jujuba seeds in the range 49.4 to 40 % with an increase in pH from 2 to 12, while the maximum CR releasing from pine cone powder (78.12 %) was achieved in aqueous solution at pH 9.2 [57]. Hence, CR adsorption on both adsorbents was mainly due to ion exchange and physical adsorption [57],[87],[120]. The appreciable amount of the dye desorbed from PKC with the use of CH_3COOH in a batch mode could be ascribed to the role of chemisorption in the uptake of CR by PKC [103].

The undesorbed portion of the dye in the sorbate could be explained by complex formation between the CR molecules and the active sites on PKC, hence accounting the inability of the eluting solvents to completely desorb the dye [103]. Mishra et al. [84] studied the desorption of CR from spent mahua oil cake using distilled water, 1M H_2SO_4 and 1N NaOH. It was observed that maximum desorption of 36 % occurred using NaOH which could be attributed to surface sites responsible for elution [84].

The desorption studies of CR loaded pomegranate rind carbon accomplished with water (neutral pH), 1M H_2SO_4 and 1M NaOH solution, however, were ineffective, while an insignificant but higher level of CR desorption with 1M CH_3COOH was achieved. Based on these results the authors supposed that the dye adsorption was predominantly attributed to chemisorption and to a lesser extent to ion exchange and physisorption [102]. Similar results were obtained by Namasivayam and Kanchana [113] who observed 5.56, 1.67 and 1.85 % of CR desorption from dye-loaded waste banana pith with distilled water, 2N H_2SO_4 and 50 % (v/v) CH_3COOH, respectively. Namasivayam and Kavitha [20] established a direct relationship between pH and the extent of CR desorption from dye-loaded coir pith carbon: the percent desorption increased from 0.5 to 10 % and from 1.2 to 11 % in the pH range 2 - 10 at C_o 20 mg L^{-1} and 40 mg L^{-1}, respectively. The latter trend suggested that chemisorption might be the major mechanism responsible for CR adsorption on coir pith activated carbon [20].

The desorption procedure in a fixed-bed column was described by the concept of an elution curve, which is also known as a desorption step. The elution curve normally has an unsymmetrical frequency distribution, with a rapid increase of the released sorbate concentration followed by a flat diminution [121]. This produces the appearance of a peak that provides two important parameters: the maximum concentration peak (C_p), which measures the eluted sorbate at this point, and the time passed until the effluent concentration peak reaches its maximum value (t_p), giving an idea of the elution rate. In the study of Oladoja and Akinlabi [103] desorption was carried out in a fixed-bed column of previously CR loaded PKC using 0.1 M CH_3COOH, the best eluting solvent, from the batch desorption studies. A rapid desorption of the sorbed CR was obtained at the inception of the studies, and this was followed by a flat diminution. The C_p was 141.46 mg L^{-1} and the t_p - 4 min. The attained elution efficiency, E 85.67 %, could be considered as high for any desorption process [103].

The same scientific team presented also a strategy for the future regeneration, reuse and utilization of the exhausted adsorbent including drying and consequent application as a fuel in boilers/incinerators, or for the production of fuel briquettes.

The bottom ash may be blended with clay to make firebricks or with a cement-concrete mixture to make coloured building blocks, thus disposing of dyes through chemical and physical fixation [103].

VI. Conclusion

The present paper highlighted the effect of some major parameters on CR adsorption by various lignocellulosic materials and visualized the following general findings: (i) The observed FTIR adsorbent spectral differences before and after adsorption: reduction in band intensities and vibration changes, indicated the possible involvement of carbonyl (–C=O), carboxyl (–COOH), hydroxyl alcocholic (–OH) and amino (–NH$_2$) functional groups on the sorbent surfaces during the adsorption process and probable interaction with the sulfonic acid (–SO$_3$H) groups of CR molecules. (ii) The fresh and dye-loaded adsorbents characterized with irregular and porous texture surface morphology. (iii) The established deviations of the pH effect could be explained by modification of the state of ionization of the binding groups, either increasing or decreasing the competition between the protonated species and adsorbate molecules for the active sites. The major mechanisms proposed in the present review include: electrostatic interactions between negatively charged dye SO$_3^-$ groups and positively charged adsorbent surfaces; H–bonding between oxygen and nitrogen containing functional groups of CR and sorbent surface; hydrophobic–hydrophobic interactions between hydrophobic parts of the dye and the sorbent. (iv) A direct relationship between the increase in the ionic strength and the positive charge of the sorbent surface leading to increased electrostatic interaction between CR molecules and some agro-industrial materials explained their increased adsorption capacity. (v) The applicability of the Langmuir and/or Freundlich models to the equilibrium experimental data for most of the sorbent/sorbate systems outlined the possibility of monolayer adsorption and/or heterogeneous energetic distribution of active sites on the sorbent surface. (vi)

The kinetic data usually followed the pseudo-second-order model. However, the role and significance of intraparticle diffusion could not be totally neglected. (vii) The thermodynamic studies indicated the spontaneous, exothermic/endothermic and physical nature of CR adsorption and suggested increased randomness at the solid/solution interface.

The current review, however, ascertained insufficient number of studies subjected to the dynamics of CR adsorption on the "eco-friendly" adsorbents in fixed-bed columns. Hence, further investigations in this scientific direction are still required to describe all aspects of the diazo dye adsorption behaviour and mechanism.

The comparative disadvantage of the low-cost adsorbents in relation to commercial activated carbons does not reduce their value as alternative adsorbent materials for CR containing wastewaters since these materials are available, low-cost: either untreated or subjected to inexpensive modification processes (heating, chemical treatment with HCl, etc), characterized with significant specific surface area and most of them exhibited satisfactory adsorption capacity (Fig. 5).
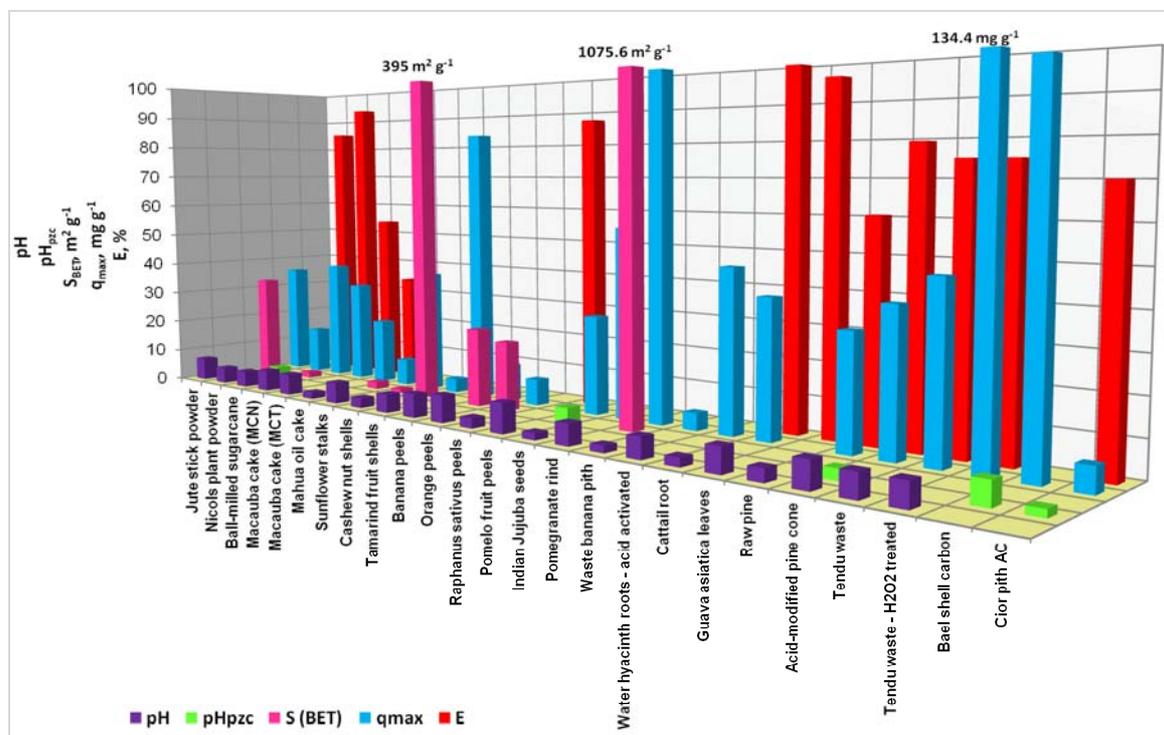

Fig. 5. Physicochemical characteristics (pH; point of zero charge, pH$_{pzc}$; BET surface area, S$_{BET}$) and adsorption properties (percent uptake, E; adsorption capacity, q$_{max}$) of various agro-industrial adsorbents during CR adsorption. Graphically presented data adapted from [10],[13],[20],[57],[83],[84],[87]-[92],[96],[97],[99],[101],[102],[111],[113],[116]

References

[1] E. Rosales, M. Pazos, M.A. Sanromán, T. Tavares, Application of zeolite-*Arthrobacter viscosu*s system for the removal of heavy metal and dye: Chromium and Azure B, *Desalination 284* (2011) 150-156.

[2] D. T. Sponza, M. Isik, Toxicity and intermediates of C.I. Direct Red 28 dye through sequential anaerobic/aerobic treatment, *Process Biochem. 40* (2005) 2735–2744.

[3] C. Cripps, J.A. Bumpus, S.D. Aust, Biodegradation of azo and heterocyclic dyes by *Phanerochaete chrysosporium*, Appl. Environ. Microbiol. 56 (4) (1990) 1114- 1118.

[4] K. Selvam, K. Swaminathan, K. Chae, Decolourization of azo dyes and a dye industry effluent by a white rot fungus *Thelephora sp.*, *Bioresource Technol. 88* (2003) 115–119.

[5] A. Pielesz, A. Weselucha-Birczynska, The identification of structural changes in the kerati of wool fibre dyed with an azo dye using Raman and Fourier transform infrared spectroscopy methods, *J. Mol. Struc. 555* (2000) 325–334.

[6] K.T. Chung, S.E. Stevens, Degradation of azo dyes by environmental microorganisms and helminits, *Environ. Toxicol. Chem. 12* (1993) 2121–2132.

[7] E.G. Snyderwine, R. Sinha, J.S. Felton, L.R. Ferguson, Higlights of the eight international conference on carcinogenic/mutagenic N-substituted aryl compounds, *Mut. Res. 506* (2002) 1–8.

[8] Dritte Verordung zur Anderung der Bedarfsgegenstandenverordnung, Bundesgesetzblatt, Jahrgang 12 (1994) Teil I.

[9] Azo Dyestuffs and ECOTEX testing for Europe STR, in http://www.erols.com/strlab/azodyes.htm.

[10] N. Rajamohan, Equilibrium studies on sorption of an anionic dye onto acid activated water hyacinth roots, *African J. Environ. Sci. Technol. 3* (11) (2009) 399-404.

[11] S.S. Vieira, Z.M. Magriotis, N.A.V. Santos, M.G. Cardoso, A.A. Saczk, Macauba palm (*Acrocomia aculeata*) cake from biodiesel processing: An efficient and low cost substrate for the adsorption of dyes, *Chem. Eng. J.* (2012), doi:10.1016/j.cej.2011.12.047.

[12] M.A.M. Salleh, D.K. Mahmoud, W.A. Wan Abdul Karim, A. Idris, Cationic and anionic dye adsorption by agricultural solid wastes: A comprehensive review, *Desalination 280* (2011) 1–13.

[13] Y.M. Slokar, A. Majcen Le Marechal, Methods of decoloration of textile wastewaters, *Dyes Pigments 37* (1998) 335-356.

[14] M.N.V. Kumar, T.R. Sridhari, K.D. Bhavani, P.K. Dutta, Trends in color removal from textile mill effluents, *Bioresource Technol. 77* (1998) 25-34.

[15] S.J. Allen, B. Koumanova, Decolourisation of water/wastewater using adsorption (review), *J. Univ. Chem. Technol. Met. (Sofia) 40* (3) (2005) 175-192.

[16] A. Demirbas, Agricultural based activated carbons for the removal of dyes from aqueous solutions: a review, *J. Hazard. Mater. 167* (2009) 1–9.

[17] A.S. Franca, L.S. Oliveira, M.E. Ferreira, Kinetics and equilibrium studies of methylene blue adsorption by spent coffee grounds, *Desalination 249* (2009) 267–272.

[18] M.A. Mumin, M.M.R. Khan, K.F. Akhter, M.J. Uddin, Potentiality of open burnt clay as an adsorbent for the removal of Congo red from aqueous solution, *Int. J. Environ. Sci. Technol. 4* (4) (2007) 525-532.

[19] L. Wang, A. Wang, Adsorption properties of congo red from aqueous solution onto N,O-carboxymethyl-chitosan, *Bioresource Technol. 99* (2008) 1403–1408.

[20] C. Namasivayam, D. Kavitha, Removal of Congo Red from water by adsorption onto activated carbon prepared from coir pith, an agricultural solid waste, *Dyes Pigments 54* (2002) 47–58.

[21] A.R. Binupriya, M. Sathishkumar, K. Swaminathan, C.S. Ku, S.E. Yun, Comparative studies on removal of Congo red by native and modified mycelial pellets of *Trametes versicolor* in various reactor modes, *Bioresource Technol. 99* (2008) 1080–1088.

[22] A. Tor, Y. Cengeloglu, Removal of congo red from aqueous solution by adsorption onto acid activated red mud, *J. Hazard. Mater. B138* (2006) 409–415.

[23] L. Wang, A. Wang, Adsorption properties of Congo Red from aqueous solution onto surfactant-modified montmorillonite, *J. Hazard. Mater. 160* (1) (2008) 173–180.

[24] H. Chen, J. Zhao, Adsorption study for removal of Congo red anionic dye using organo-attapulgite, *Adsorption 15* (2009) 381–389.

[25] Z. Zhang, Y. Shan, J. Wang, H. Ling, S. Zang, W. Gao, Z. Zhao, H. Zhang, Investigation on the rapid degradation of congo red catalyzed by activated carbon powder under microwave irradiation, *J. Hazard. Mater. 147* (1-2) (2007) 325-333.

[26] R.H.S.V. Vieira, B.Volesky, Biosorption - a solution to pollution? *Int. Microbiol. 3* (2000) 17-24.

[27] U. Farooq, M.A. Khan, W. Athar, J.A. Kozinski, Effect of modification of environmentally friendly biosorbent wheat (*Triticum aestivum)* on the biosorptive removal of cadmium (II) ions from aqueous solution, *Chem. Eng. J. 171* (2011) 400-410.

[28] R.W. Sabnis, *Handbook of Biological Dyes and Stains. Synthesis and Industrial Applications* (John Wiley & Sons, New Jersey, Canada, Springer, 2010, pp. 106-107).

[29] S. Chatterjee, S. Chatterjee, B.P. Chatterjee, A.K. Guha, Adsorptive removal of congo red, a carcinogenic textile dye by chitosan hydrobeads: Binding mechanism, equilibrium and kinetics, *Colloid Surface A 299* (1–3) (2007) 146–152.

[30] V. Vimonses, S. Lei, B. Jin, C.W.K. Chow, C. Saint, Kinetic study and equilibrium isotherm analysis of Congo Red adsorption by clay materials, *Chem. Eng. J. 148* (2009) 354–364.

[31] M.K. Purkait, A. Maiti, S.D. Gupta, S. De, Removal of congo red using activated carbon and its regeneration, *J. Hazard. Mater. 145* (2007) 287–295.

[32] R. Han, D. Ding, Y. Xu, W. Zou, Y. Wang, Y. Li, L. Zou, Use of rice husk for the adsorption of congo red from aqueous solution in column mode, *Bioresource Technol. 99* (2008) 2938–2946.

[33] A.S. Raymundo, R. Zanarotto, M. Belisário, M.G. Pereira, J.N. Ribeiro, A.V.F.N. Ribeiro, Evaluation of sugar-cane bagasse as bioadsorbent in the textile wastewater treatment contaminated with carcinogenic congo red dye, *Brazilian Arch. Biology Technol. 53* (4) (2010) 931-938.

[34] A. Pielesz, The process of the reduction of azo dyes used in dyeing textiles on the basis of infrared spectroscopy analysis, *J. Mol. Struct. 511-512* (1999) 337–44.

[35] H.M. Pinheiro, E. Touraud, O. Thomas, Aromatic amines from azo dye reduction: status review with emphasis on direct UV spectrophotometric detection in textile industry wastewaters, *Dyes Pigments 61* (2004) 121–139.

[36] C. Smaranda, M. Gavrilescu, D. Bulgariu, Studies on sorption of Congo Red from aqueous solution onto soil, *Int. J. Environ. Res. 5* (1) (2011) 177-188.

[37] J.M. Chern, Y.W. Chien, Adsorption of nitrophenols onto activated carbon: isotherms and breakthrough curves, *Wat. Res. 36* (2002) 647-655.

[38] P. Gharbani, S.M. Tabatabaii, A. Mehrizad, Removal of Congo red from textile wastewater by ozonation, *Int. J. Environ. Sci. Technol. 5* (4) (2008) 495-500.

[39] M.F. Elahmadia, N. Bensalahb, A. Gadria, Treatment of aqueous wastes contaminated with Congo Red dye by electrochemical oxidation and ozonation processes, *J. Hazard. Mater. 168* (2009) 1163–1169.

[40] P. Suwannawong, S. Khammuang, R. Sarnthima, Decolorization of rhodamine B and congo red by partial purified laccase from *Lentinus polychrous Lév*, *J. Biochem. Technol. 3* (2) (2010) 182-186.

[41] A. López–Vásquez, D. Santamaría, M. Tibatá, C. Gómez, Congo red photocatalytic decolourization using modified titanium, *World Academy of Science, Engineering and Technology 71* (2010) 122-125.

[42] R.K. Wahi, W. Yu, Y. Liu, M.L. Mejia, J.C. Falkner, W. Nolte, V.L. Colvin, Photodegradation of Congo Red catalyzed by nanosized TiO_2, *J. Mol. Catal. A-Chem. 242* (2005) 48–56.

[43] H. Zhua, R. Jiang, L. Xiao, Y. Chang, Y. Guan, X. Li, G. Zeng, Photocatalytic decolorization and degradation of Congo Red on innovative crosslinked chitosan/nano-CdS composite catalyst under visible light irradiation, *J. Hazard. Mater. 169* (2009)

933–940.

[44] D. Kamel, A. Sihem, C. Halima, S. Tahar, Decolourization process of an azoique dye (Congo red) by photochemical methods in homogeneous medium, *Desalination 250* (2009) 76–86.

[45] S.P. Meshram, D.T. Tayade, P.D. Ingle, P.D. Jolhe, B.B. Diwate, S.B. Biswas, Ultrasonic cavitation induced degradation of Congo Red in aqueous solutions, *Chem. Eng. Res. Bulletin 14* (2010) 119-123.

[46] S. Sistla, S. Chintalapati, Sonochemical degradation of Congo Red, Int. J. Environ. Waste Manage. 2 (3) 2008 309 - 319.

[47] N.D. Zhang, Z. Zhu, W. Luan, Degradation mechanism of acidic Congo Red in sunlight/Fe^{2+}/$S_2O_8^{2-}$ system, *Acta Chim. Sinica 69* (19) (2011) 2307-2312.

[48] A. Telke, S. Joshi, S. Jadhav, D. Tamboli, S.P. Govindwar, Decolorization and detoxification of Congo red and textile industry effluent by an isolated bacterium *Pseudomonas sp. SU-EBT*, *Biodegradation 21* (2010) 283–296.

[49] U. Ogutveren, S. Koparal, Electrochemical treatment of water containing dye-stuffs: anodic oxidation of congo red and xiron blau 2RHD, *Int. J. Environ. Stud. 42* (1) (1992) 41-52.

[50] C. Wang, Decolorization of Congo Red with three-dimensional flow-by packed-bed electrodes, *J. Environ. Sci. Heal. A 38* (2) (2003) 399-413.

[51] A. Kondru, P. Kumar, S. Chand, Catalytic wet peroxide oxidation of azo dye (Congo red) using modified Y zeolite as catalyst, *J. Hazard. Mater. 166* (2009) 342–347.

[52] H. Patel, R.T. Vashi, Removal of Congo Red dye from its aqueous solution using natural coagulants, *J. Saudi Chem. Society* (2011), doi:10.1016/j.jscs.2010.12.003.

[53] T.K. Sen, S. Afroze, H.M. Ang, Equilibrium, kinetics and mechanism of removal of methylene blue from aqueous solution by adsorption onto pine cone biomass of *Pinus radiate*, *Water Air Soil Poll. 218* (2011) 499-515.

[54] Z. Yao, Z., L. Wang, J. Qi, Biosorption of methylene blue from aqueous solution using a bioenergy forest waste: *Xanthoceras sorbifolia* seed coat, *Clean 37* (8) (2009) 642-648.

[55] M.M. Abd El-Latif, A.M. Ibrahim, M.F. El-Kady, Adsorption equilibrium, kinetics and thermodynamics of methylene blue from aqueous solutions using biopolymer oak sawdust composite, *J. Am. Sci. 6* (6) (2010) 267-283.

[56] M. Ghaedi, J. Tashkhourian, A.A. Pebdani, B. Sadeghian, F.N. Ana, Equilibrium, kinetic and thermodynamic study of removal of reactive orange 12 on platinum nanoparticle loaded on activated carbon as novel adsorbent, *Korean J. Chem. Eng. 28* (12) (2011) 2255-2261.

[57] S. Dawood, T.K. Sen, Removal of anionic dye Congo red from aqueous solution by raw pine and acid-treated pine cone powder as adsorbent: Equilibrium, thermodynamic, kinetics, mechanism and process design, *Water Res. 46* (6) (2012) 1933-1946.

[58] S. Nouri, F. Haghsereht, G.Q. Max Lu, Comparison of the adsorption capacity of p-cresol and p-nitrophenol by activated carbon in single and double solute, *Adsorption 8* (2002) 215-223.

[59] B. Koumanova, Z. Yaneva, Low-cost adsorbents for the removal of nitrophenols from waste waters, *Management of Intentional and Accidental Water Pollution* (Springer, 2006, G. Dura et al. (eds.), Netherlands, pp. 263–275).

[60] V. Vimonses, S. Lei, B. Jin, C.W.K. Chow, C. Saint, Adsorption of congo red by three Australian kaolins, *Appl. Clay Sci. 43* (2009) 465–472.

[61] L. Lian, L. Guo, A. Wang, Use of $CaCl_2$ modified bentonite for removal of Congo red dye from aqueous solutions, Desalination 249 (2009) 797–801.

[62] E. Bulut, M. Ozacar, I.A. Sengil, Equilibrium and kinetic data and process design for adsorption of Congo Red onto bentonite, *J. Hazard. Mater. 154* (2008) 613–622.

[63] M. Toor, B. Jin, Adsorption characteristics, isotherm, kinetics, and diffusion of modified natural bentonite for removing diazo dye, *Chem. Eng. J.* (2012), doi:10.1016/j.cej.2012.01.089.

[64] V. Vimonses, B. Jin, C. W.K. Chow, Insight into removal kinetic and mechanisms of anionic dye by calcined clay materials and lime, *J. Hazard. Mater. 177* (2010) 420–427.

[65] Y. Yang, G. Wang, B. Wang, Z. Li, X. Jia, Q. Zhou, Y. Zhao, Biosorption of Acid Black 172 and Congo Red from aqueous solution by nonviable Penicillium YW 01: Kinetic study, equilibrium isotherm and artificial neural network modeling, *Bioresource Technol. 102* (2011) 828–834.

[66] E. Lorenc-Grabowska, G. Gryglewicz, Adsorption characteristics of Congo Red on coal-based mesoporous activated carbon, *Dyes Pigments 74* (2007) 34-40.

[67] R. Jayaraj, P.J. Thanaraj, S.T. Natarajan, P.M.D. Prasath, Removal of Congo red dye from aqueous solution using acid activated eco-friendly low cost carbon prepared from marine algae *Valoria bryopsis*, *J. Chem. Pharm. Res. 3* (3) (2011) 389-396.

[68] H.Y. Zhu, Y.Q. Fu, R. Jiang, J.H. Jiang, L. Xiao, G.M. Zeng, S.L. Zhao, Y. Wang, Adsorption removal of congo red onto magnetic cellulose/Fe_3O_4/activated carbon composite: Equilibrium, kinetic and thermodynamic studies, *Chem. Eng. J. 173* (2011) 494-502.

[69] M. Ghaedi, M.N. Biyareh, S.N. Kokhdan, S.H. Shamsodini, R. Sahraei, A. Daneshfar, S. Shahriyara, Comparison the efficiency of Palladium and Silver nanoparticle loaded on activated carbon and Zinc oxide nanorods loaded on activated carbon as new adsorbents for removal of Congo red from aqueous solution: Kinetic and isotherm study, *Mat. Sci. Eng. C* (2012), doi: 10.1016/j.msec.2012.01.015.

[70] B. Cheng, Y. Le, W. Cai, J. Yu, Synthesis of hierarchical $Ni(OH)_2$ and NiO nanosheets and their adsorption kinetics and isotherms to Congo red in water, *J. Hazard. Mater. 185* (2011) 889–897.

[71] C. Namasivayam, R.T. Yamuna, Removal of congo red from aqueous solutions by biogas waste slurry, *J. Chem. Technol. Biot. 53* (2) (1992) 153–157.

[72] C. Namasivayam, D.J.S.E. Arasi, Removal of congo red from wastewater by adsorption onto waste red mud, *Chemosphere 34* (2) (1997) 401–417.

[73] A.K. Golder, A.N. Samanta, S. Ray, Anionic reactive dye removal from aqueous solution using a new adsorbent—Sludge generated in removal of heavy metal by electrocoagulation, *Chem. Eng. J. 122* (2006) 107–115.

[74] M.A. Islam, V. Sakkas, T. Albanis, Sorption-desorption of an azo dye on different Greek soils, *Proceedings of the 11th International Conference on Environmental Science and Technology. Creete, Greece, pp. B-382 - B-387, 3-5 Sept (2009)*.

[75] L. Wang, A. Wang, Adsorption characteristics of Congo Red onto the chitosan/montmorillonite nanocomposite, *J. Hazard. Mater. 147* (2007) 979–985.

[76] C. Namasivayam, R. Jeyakumar, R.T. Yamuna, Dye removal from wastewater by adsorption on 'waste' Fe(III)/Cr(III) hydroxide, *Waste Manage. 14* (7) (1994) 643–648.

[77] L. Wang, J. Li, Y. Wang, L. Zhao, Q. Jiang, Adsorption capability for Congo red on nanocrystalline MFe_2O_4 (M = Mn, Fe, Co, Ni) spinel ferrites, *Chem. Eng. J. 181-182* (2011) 72-79.

[78] P.D. Saha, S. Chowdhury, M. Mondal, K. Sinha, Biosorption of Direct Red 28 (Congo Red) from aqueous solutions by eggshells: Batch and column studies, *Separ. Sci. Technol. 47 (1)* (2012) 112-123.

[79] F.A. Pavan, S.L.P. Dias, E.C. Lima, E.V. Benvenutti, Removal of Congo red from aqueous solution by anilinepropylsilica xerogel, *Dyes Pigments 76* (2008) 64-69.

[80] L. Nadjia, E. Abdelkader, B. Ahmed, Photodegradation study of Congo Red in Aqueous Solution using ZnO/UV-A: Effect of pH and Band Gap of other Semiconductor Groups, J. *Chem. Eng. Process. Technol. 2* (108) (2011), doi:10.4172/2157-7048.1000108.

[81] M. Movahedi, A.R. Mahjoub, S. Janitabar-Darzi, Photodegradation of Congo Red in Aqueous Solution on ZnO as an Alternative Catalyst to TiO_2, *J. Iran. Chem. Soc. 6* (3) (2009) 570-577.

[82] C.E. Bonancea, G.M. do Nascimento, M.L. de Souza, M.L.A. Temperini, P. Corio, Substrate development for surface-enhanced Raman study of photocatalytic degradation processes:

Congo red over silver modified titanium dioxide films, *Appl. Catal. B - Environ. 69* (2006) 34–42.

[83] R. Ahmad, R. Kumar, Adsorptive removal of congo red dye from aqueous solution using bael shell carbon, Appl. Surf. Sci. 257 (2010) 1628-1633.

[84] S. Mishra, D.J. Prakash, G. Ramakrishna, Characterization and utilization of Mahua oil cake - A new adsorbent for removal of Congo red dye from aqueous phase, *EJEAFChe. 8* (6) (2009) 425-436.

[85] R. Han, Y. H. Li, H. Q. Li, Y.J. Wu, J. Shi, The elemental analysis and FT-IR comparison between MDP and casting. *Spectrosc. Spect. Anal. 24* (suppl.) (2004) 185–186.

[86] D. Sarkar, A. Bandyopadhyay, Shrinking Core Model in characterizing aqueous phase dye adsorption, *Chem. Eng. Res. Des. 89* (2011) 69–77.

[87] M.C. Somasekhara Reddy, L. Sivaramakrishna, A. Varada Reddy, The use of an agricultural waste material, Jujuba seeds for the removal of anionic dye (Congo red) from aqueous medium, *J. Hazard. Mater. 203–204* (2012) 118–127.

[88] G.C. Panda, S.K. Das, A.K. Guha, Jute stick powder as a potential biomass for the removal of congo red and rhodamine B from their aqueous solution, *J. Hazard. Mater. 164 (2009) 374–379.*

[89] A.K. Patil, V.S. Shrivastava, *Alternanthera bettzichiana* plant powder as low cost adsorbent for removal of Congo red from aqueous solution, *Int. J. Chem. Tech. Res. 2* (2) (2010) 842-850.

[90] K.G. Bhattacharyya, A. Sharma, *Azadirachta indica* leaf powder as an effective biosorbent for dyes: a case study with aqueous Congo red solutions, *J. Environ. Manage. 71* (3) (2004) 217–229.

[91] P.S. Kumar, S. Ramalingam, C. Senthamarai, M. Niranjanaa, P. Vijayalakshmi, S. Sivanesan, Adsorption of dye from aqueous solution by cashew nut shell: Studies on equilibrium, isotherm, kinetics and thermodynamics of interactions, *Desalination 261* (2010) 52–60.

[92] Z. Hu, H. Chen, F. Ji, S. Yuan, Removal of Congo Red from aqueous solution by cattail root, *J. Hazard. Mater. 73* (2010) 292–297.

[93] H.C. Tee, C.E. Seng, A.M. Noor, P.E. Lim, Performance comparison of constructed wetlands with gravel- and rice husk-based media for phenol and nitrogen removal, *Sci. Total Environ. 407* (2009) 3563–3571.

[94] S. Kantawanichkul, S. Kladprasert, H. Brix, Treatment of high-strength wastewater in tropical vertical flow constructed wetlands planted with *Typha angustifolia* and *Cyperus involucratus*, *Ecol. Eng. 35* (2009) 238–247.

[95] M.P. Ciria, M.L. Solano, P. Soriano, Role of macrophyte *Typha latifolia* in a constructed wetland for wastewater treatment and assessment of its potential as a biomass fuel, *Biosyst. Eng. 92* (2005) 535–544.

[96] G. Annadurai, R. Juang, D. Lee, Use of cellulose-based wastes for adsorption of dyes from aqueous solutions, *J. Hazard. Mater. B92* (2002) 263–274.

[97] Z. Zhang, L. Moghaddam, I.M. O'Hara, W.O.S. Doherty, Congo Red adsorption by ball-milled sugarcane bagasse, *Chem. Eng. J. 178* (2011) 122– 128.

[98] A.S. Raymundo, R. Zanarotto, M. Belisário, M.G. Pereira, J.N. Ribeiro, A.V.F.N. Ribeiro, Evaluation of sugar-cane bagasse as bioadsorbent in the textile wastewater treatment contaminated with carcinogenic congo red dye, *Brazilian Arch. Biology Technol. 53* (4) (2010) 931-938.

[99] D.A. Naidu, P. Vijay, P. King, V.S.R.K. Prasad, Biosorption of congo red from aqueous solution using Guava (*Psidium Guajava*) leaf powder: Equilibrium and kinetic studies, *The IUP Journal of Chemical Engineering 2* (1) (2010) 27-45.

[100] R.A. Carletto, F. Chimirri, F. Bosco, F. Ferrero, Adsorption of congo red dye on hazelnut shells and degradation with *Phanerochaete chrysosporium*, *BioResources 3* (4) (2008) 1146-1155.

[101] R. Rehman, A. Abbas, S. Murtaza, T. Mahmud, W. Zaman, M. Salman, U. Shafique, Comparative removal of congo red dye from water by adsorption on *Grewia asiatica* leaves, *Raphanus*

sativus peels and activated charcoal, *J. Chem. Soc. Pak. 34* (1) (2012) 112-119.

[102] R. Venckatesh, T. Amudha, R. Sivaraj, M. Chandramohan, M. Jambulingam, Kinetics and equilibrium studies on adsorption of Direct red-28 onto *Punica granatum* carbon, *Int. J. Eng. Sci. Technol. 2* (6) (2010) 2040-2050.

[103] N.A. Oladoja, A.K. Akinlabi, Congo red biosorption on palm kernel seed coat, *Ind. Eng. Chem. Res. 48* (13) (2009) 6188–6196.

[104] C. Gunnarsson, C.M. Petersen, Water hyacinths as a resource in agriculture and energy production: A literature review, *Waste Manage. 27* (2007) 117–129.

[105] G. Sun, X. Xu, Sunflower stalks as adsorbents for color removal from textile wastewater, Ind. Eng. Chem. Res. 36 (3) (1997) 808–812.

[106] W. Shi, X. Xu, G. Sun, Chemically modified sunflower stalks as adsorbents for color removal from textile wastewater, *J. Appl. Polym. Sci.* 71 (1999) 1841–1850.

[107] W.E. Rashwan, B.S. Girgis, Adsorption capacities of activated carbons derived from rice straw and water hyacinth in the removal of organic pollutants from water, *Adsorpt. Sci. Technol. 22* (2004) 181-194.

[108] N.A. Oladoja, A.K. Akinlabi, Congo red biosorption on palm kernel seed coat, *Ind. Eng. Chem. Res. 48* (13) (2009) 6188–6196.

[109] A.E. Ofomaja, E.B. Naidoo, Biosorption of copper from aqueous solution by chemically activated pine cone:A kinetic study, *Chem. Eng. J. 175* (2011) 260-270.

[110] R. Sivaraj, C. Namasivayam, K. Kadirvelu, Orange peel as an adsorbent in the removal of Acid violet 17 (acid dye) from aqueous solutions, *Waste Manage. 21* (2001) 105–110.

[111] M.C.S. Reddy, Removal of direct dye from aqueous solution with an adsorbent made from tamarind fruit shell, an agricultural solid waste, *J. Sci. Ind. Res. India 65* (2006) 443-446.

[112] S.S. Reddy, S.K. Bhaduri, S.K. Sen, Infrared spectra of alkali treated jute stick, *J. Appl. Polym. Sci. 41* (1990) 329–336.

[113] C. Namasivayam, N. Kanchana, Removal of Congo red from aqueous solution by waste banana pith, *Pertanika J. Sci. Technol. 1 (1)* (1993) 33-42.

[114] A. Abbas, S. Murtaza, M. Munir, Removal of congo red from aqueous solutions with *Raphanus sativus* peels and activated carbon: A comparative study, *American-Eurasian J. Agricult. Environ. Sci. 10* (5) (2011) 802-809.

[115] M. Jayarajan, R. Arunachalam, G. Annadurai, Use of low cost nano-porous materials of pomelo fruit peel wastes in removal of textile dye, *Res. J. Environ. Sci. 5* (5) (2011) 434-443.

[116] G.K. Nagda, V.S. Ghole, Biosorption of congo red by hydrogen peroxide treated tendu waste, *Iran. J. Environ. Health. Sci. Eng. 6* (3) (2009) 195-200.

[117] Z. Qi, X. Chuanxin, G. Wenqi, Z. Wenjun, Comments on the method of using maximum absorption wavelength to calculate Congo red solution concentration published in *J. Hazard. Mater. 198* (2011) 381– 382.

[118] Z. Yaneva, M. Marinkovski, L. Markovska, V. Meshko, B. Koumanova, Dynamic studies of nitrophenols sorption on perfil in a fixed-bed column, *Macedonian J. Chem. Chem. Eng. 27* (2) (2008) 123–132.

[119] D. Mall, V.C. Srivastava, G.V.A. Kumar, I.M. Mishra, Characterisation and utilization of mesoporous fertilizer plant waste carbon for adsorptive removal of dyes from aqueous solution. *Colloid Surface A 278* (2006) 175–187.

[120] H.M. Asfour, M.M. Nassar, D.A. Fadali, M.S. Ei-Geundi, Colour removal from textile effluents using hardwood saw dust as an adsorbent, *J. Chem. Technol. Biot. 35* (1985) 28–35.

[121] P. Loidero, R. Herrero, M.E. Sastra de Vicente, Batch desorption studies and multiple sorption-regeneration cycles in a fixed-bed column for Cd (II) elimination by protonated sargassum muticum. *J. Hazard. Mater. B137* (2006) 1649–1655.

Authors' information

Chemistry Unit, Department of Pharmacology, Animal Physiology and Physiological Chemistry, Faculty of Veterinary Medicine, Trakia University, Students Campus, 6000 Stara Zagora, Bulgaria

Zvezdelina Yaneva gained her PhD in chemical engineering (Processes and apparatus in the chemical and biochemical technology) from the University of Chemical Technology and Metallurgy, Sofia, Bulgaria, in 2009. Currently, she is an assistant professor in Chemistry Unit, Trakia University, Bulgaria. Her research interests are in adsorption of organic compounds from aqueous medium, mass transfer modeling, wastewater treatment, ecological monitoring and assessment of fresh waters.

Tel.: (+359) 42 699 642
Fax: (+359) 42 672 009
E-mail: z.yaneva@abv.bg

Nedyalka Georgieva gained her PhD in ecology and ecosystems ("Investigation on the influence of newly synthesized derivatives of the isonicotinic acid on oxidative stress parameters") from Trakia University, Stara Zagora, Bulgaria. Currently, she is an associate professor in Chemistry Unit, Trakia University, Bulgaria. Her main research interests are in ecological monitoring and assessment of fresh waters, wastewater treatment, synthesis of biologically active substances, influence of oxidative stress and some antioxidant enzymes on the ecological oxidative balance of living organisms. She is a member of the Union of Scientists in Bulgaria.

E-mail: nvgeorgieva@vmf.uni-sz.bg